# Transport properties of recent discovered Weyl semimetals

Chenglong Zhang[1], Hong Lu[1], Zhujun Yuan[1], Cheng Guo[1], Xiao Zhang[1], Shuang Jia[1,2]

[1]ICQM, School of Physics, Peking University

[2]Collaborative Innovation Center of Quantum Matter

4/10/2015

# Collaborators:

Bingbing Tong, Chi Zhang

Su-yang Xu, Ilya Beloposki, Nasser Alidoust, Daniel Sanchez, Madhab Neupane, Titus Neupert, Zahid Hasan

Tay-Rong Chang & Horng-Tay Jeng

Shin-Ming Huang, Chi-Cheng Lee, Guoqing Chang, Hsin Lin

Ziquan Lin, Junfeng Wang

# Introduction of Our Lab

Sample synthesis (single crystal growth)


Physical properties measurement

# OUTLINE

- Introduction of Weyl Semimetals
  - Band structure: surface Fermi arcs and bulk Weyl nodes
  - Chiral anomaly and other unique properties
- Theoretical Proposals of Weyl Semimetals
- Observation of the Weyl Semimetals in non-central-symmetric compounds
  - $Ag_2Se$
  - TaAs and Isostructural Compounds
    - Band structure calculation
    - ARPES
    - Transport properties
- Summary and Plan

# Weyl fermion: massless "Half" Dirac fermion

The Chirality of a massless fermion can be defined as:

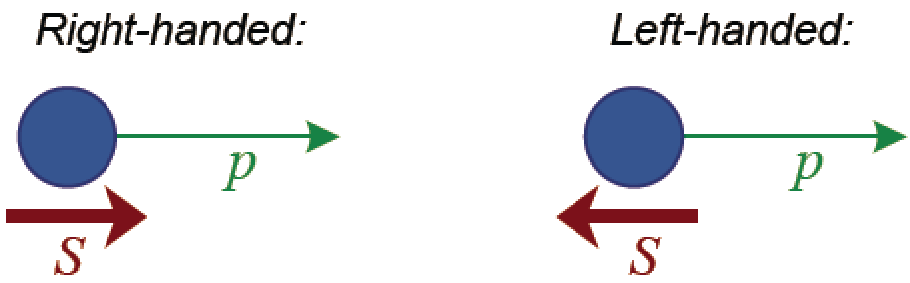


*A Dirac fermion is chiral symmetric: it can be seen as the sum of a pair of Weyl fermion*

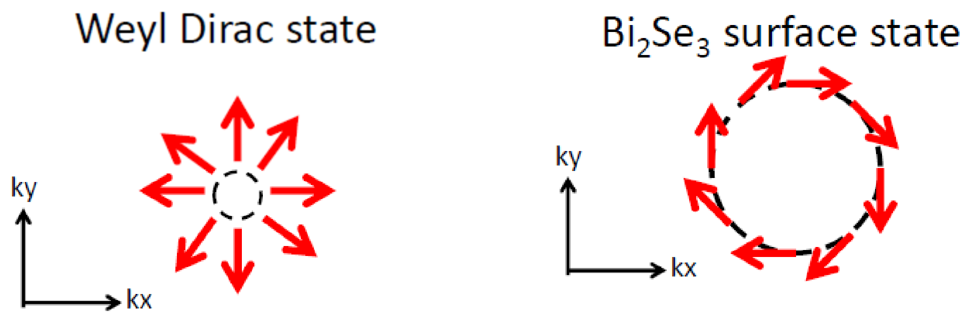


No Weyl fermion has been confirmed in high energy physics.
*However, we can study it in condensed matter physics*

# Weyl semimetal: zero-gap semimetal with certain pairs of Weyl nodes

**Weyl semimetal**

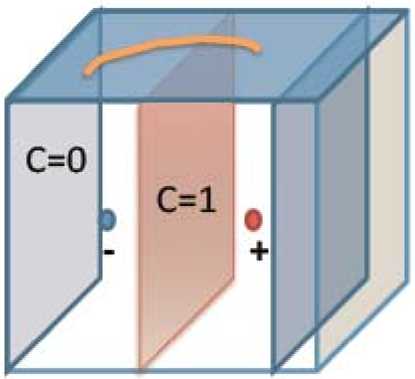


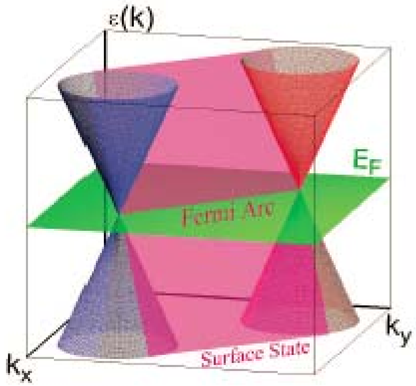


$$H = v\vec{\sigma} \cdot \vec{k}$$

Weyl semimetal has a pair of Weyl nodes with opposite chirality

**Graphene**

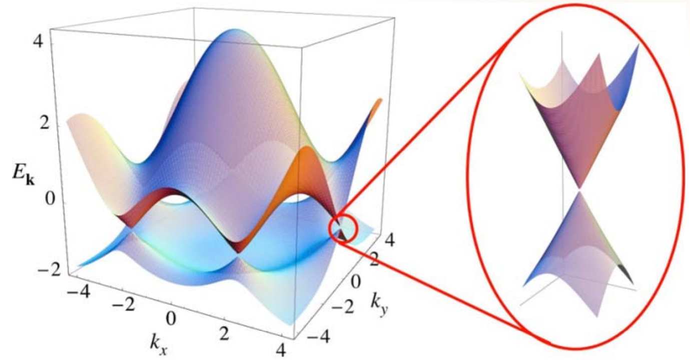


Band structure of graphene has six Dirac points

- Pairs of bands crossing at certain points (like graphene)
- The Weyl nodes are spin single degenerate. (spin textures are different)
- Fermi surface surrounding the Weyl nodes are topologically non-trivial
- The Weyl nodes with opposite chirality are connected by Fermi arcs on surfaces

# Comparison: 3D Dirac Semimetals

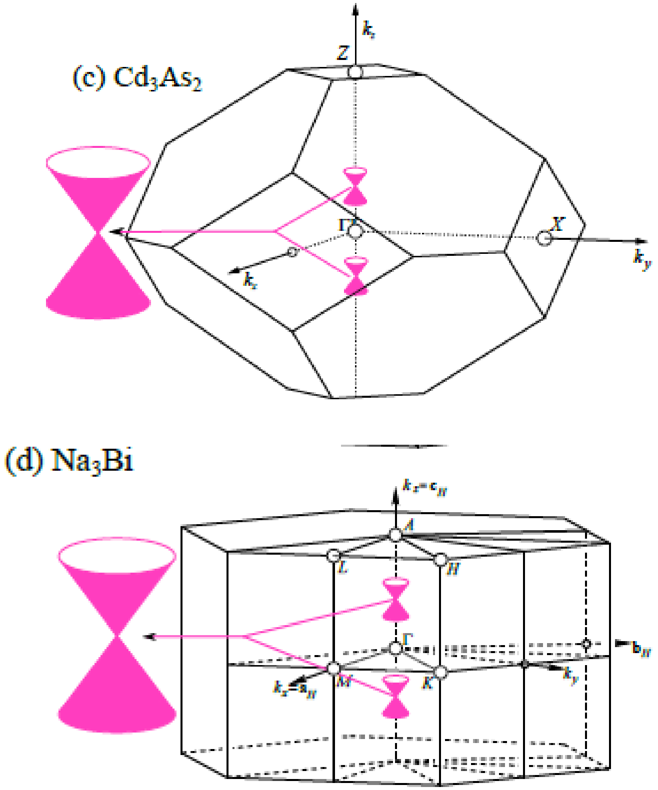


- Dirac nodes along the high-symmetry lines
- Protected by rotation symmetry
- 3D analog of graphene

Difference with Weyl points

- Degeneracy
- Spin texture near the nodes
- Position in k space

*Realization of a Weyl semimetal needs breaking a time-reversal symmetry or inversion symmetry*

# Chiral Anomaly: Negative MR

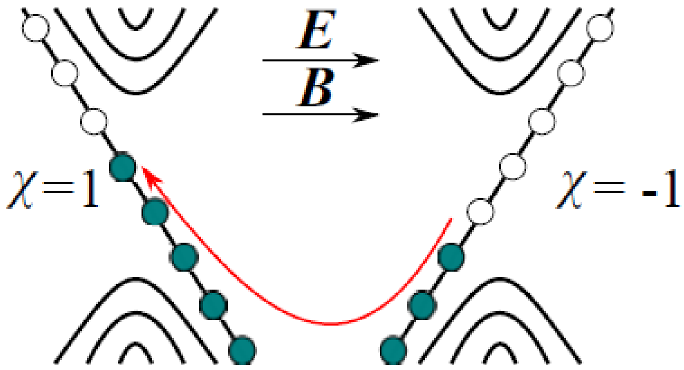


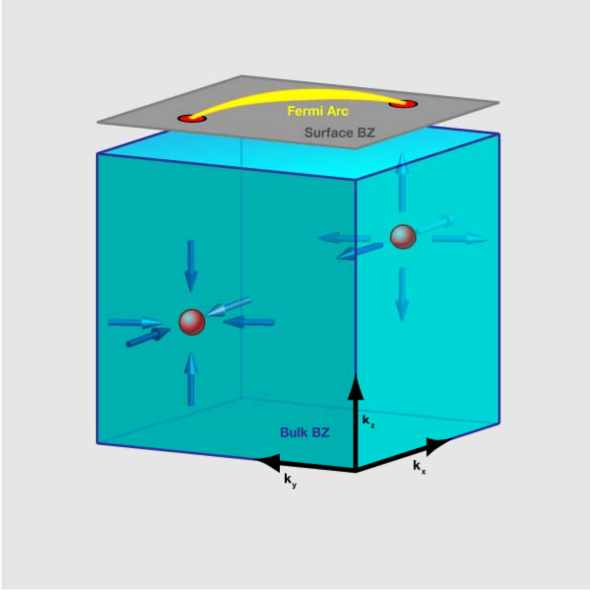


In a large field:
Beyond QL: 1D chiral anomaly
Charge pumping effect:

$$DOS \propto \vec{E} \cdot \vec{B} \propto \sigma$$

Linear positive longitudinal magneto-conductance

More general case:
Negative MR

D. Son & B. Spivak PRB 88 104412 (2013)

# How to Realize a Weyl Semimetal (Proposal I)

- A QCP realized by tuning the SOC interaction.

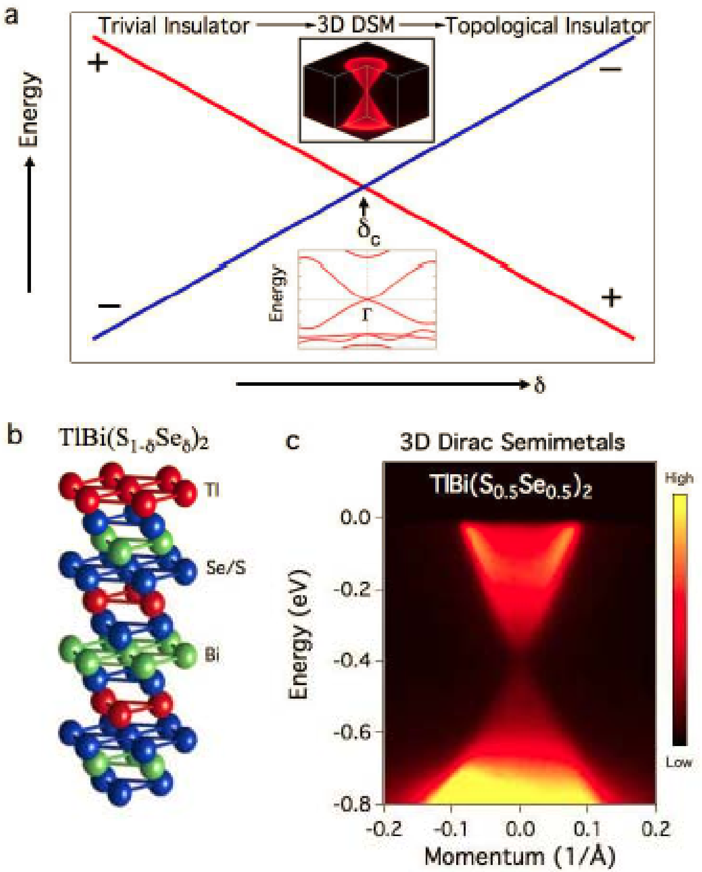


Example: $TlBi(S_{1-x}Se_x)_2$, $Bi_{1-x}Sb_x$, $Bi_{2-x}In_xSe_3$

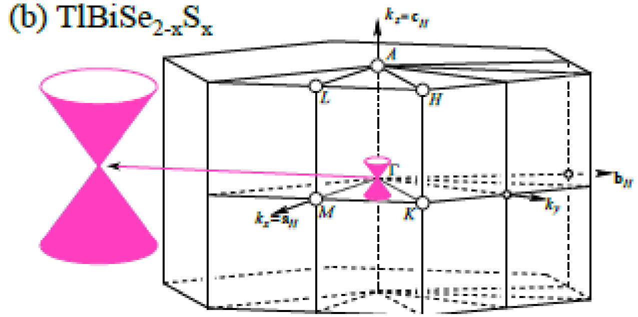


Disadvantage: doping induced disorder, need magnetic ground state

# How to Realize a Weyl Semimetal (Proposal II)

- A magnetic ordered ground state with strong spin-orbital coupling.

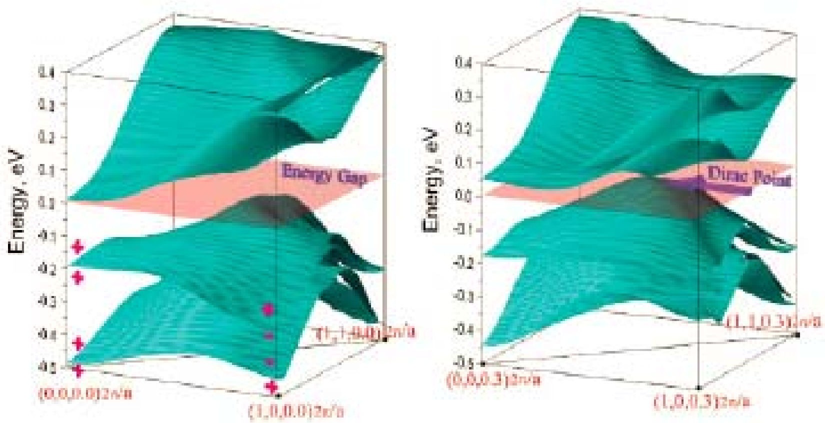


Band structure of $Y_2Ir_2O_7$
X. *Wan etal.* PRB 83 205101(2011)

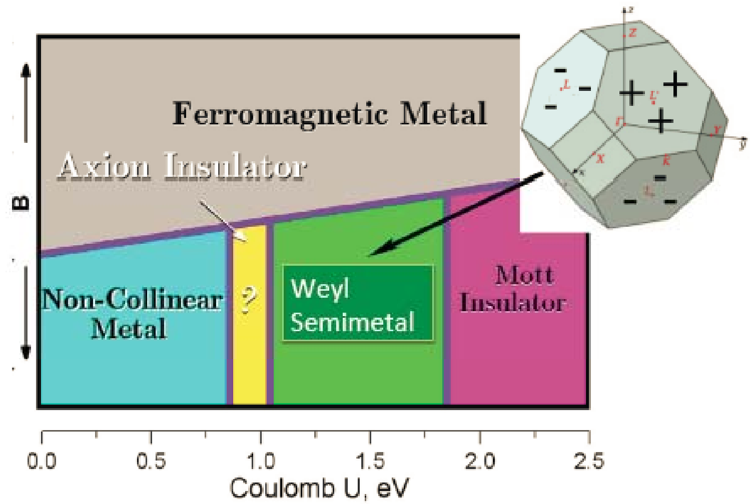


Calculated phase diagram of $Y_2Ir_2O_7$ with interaction strength
X. *Wan etal.* PRB 83 205101(2011)

Example:;$Y_2Ir_2O_7$( geometric frustrated)
Disadvantage: difficulty of sample growth, unknown magnetic structure

# How to Realize a Weyl Semimetal (Proposal II)

- A magnetic ordered ground state with strong spin-orbital coupling.

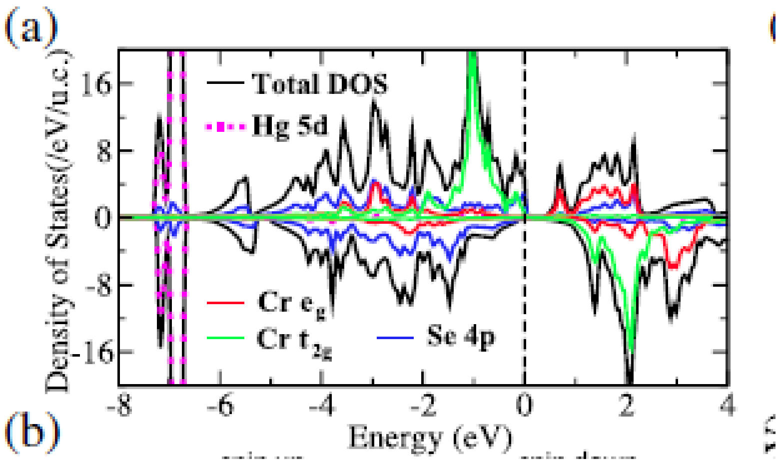


Band structure of $HgCr_2Se_4$
G. *Xu etal.* PRL 107 186806(2011)

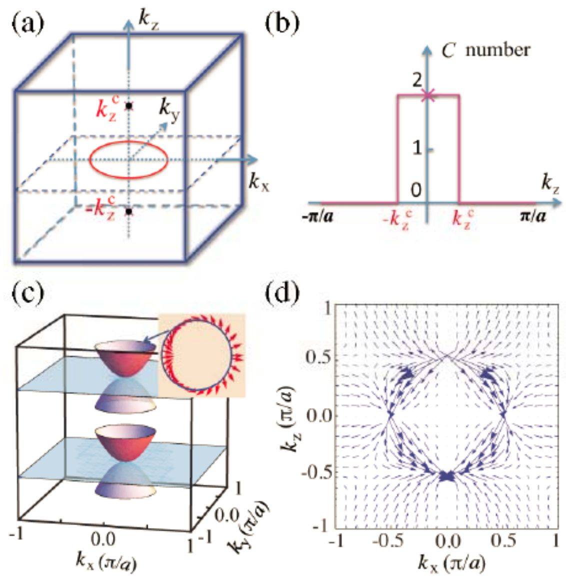


Weyl nodes in $HgCr_2Se_4$
G. *Xu etal.* PRL 107 186806(2011)

Example: $HgCr_2Se_4$ (FM spinel)
Disadvantage: difficulty of sample growth, magnetic domain

# How to Realize a Weyl Semimetal (Proposal III)

◆non-central-symmetric semimetal with proper SOC

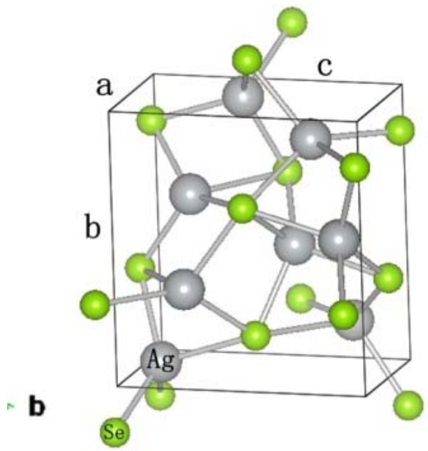


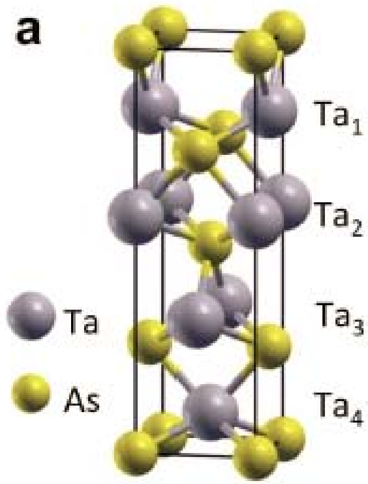


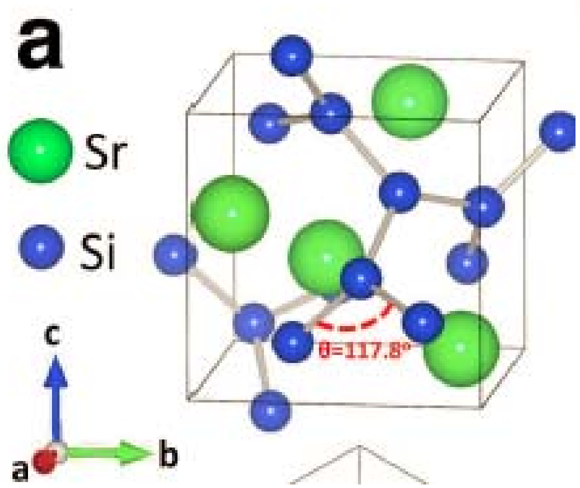


$Ag_2Se$: $P2_12_12_1$

TaAs: $I4_1md$

$SrSi_2$: $P4_332$

Difficulty:

- choose right systems (need more calculations, structural information)
- single crystal growth (thermally unstable low-T phases)

# Band Structure of $Ag_2Se$

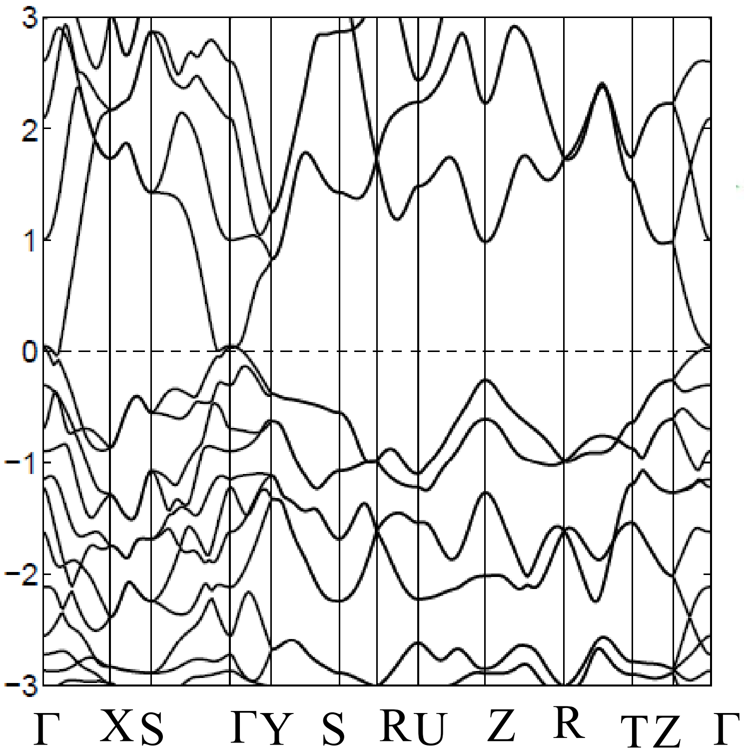


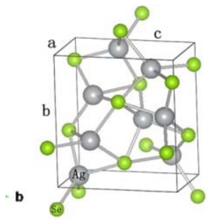


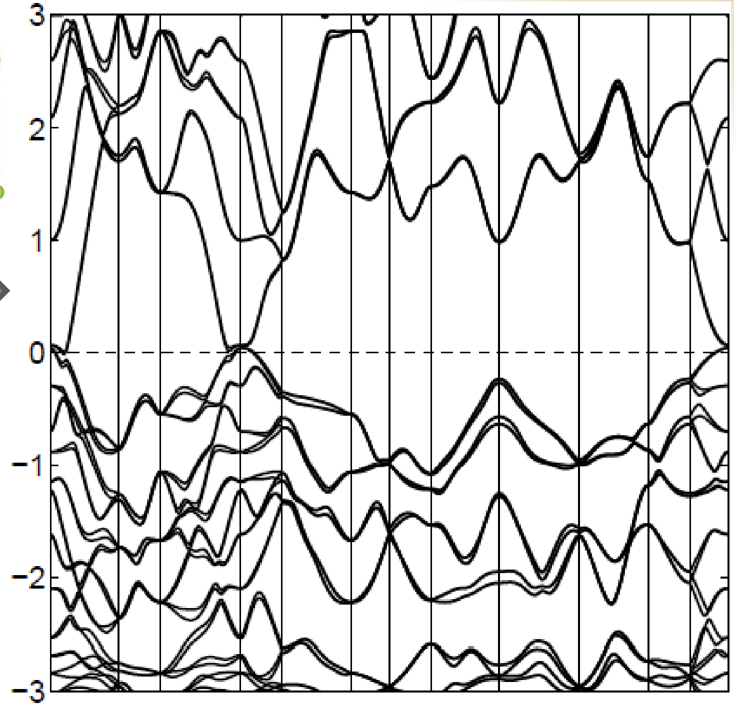


With no SOC: gapless in high-symmetry points

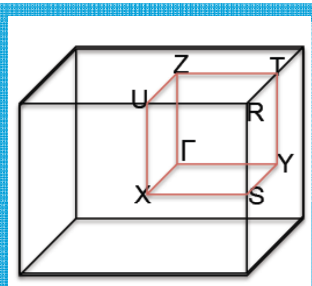


With SOC: small gap in all high-symmetry points and lines

Space group $P2_12_12_1$

# Weyl Nodes in $Ag_2Se$

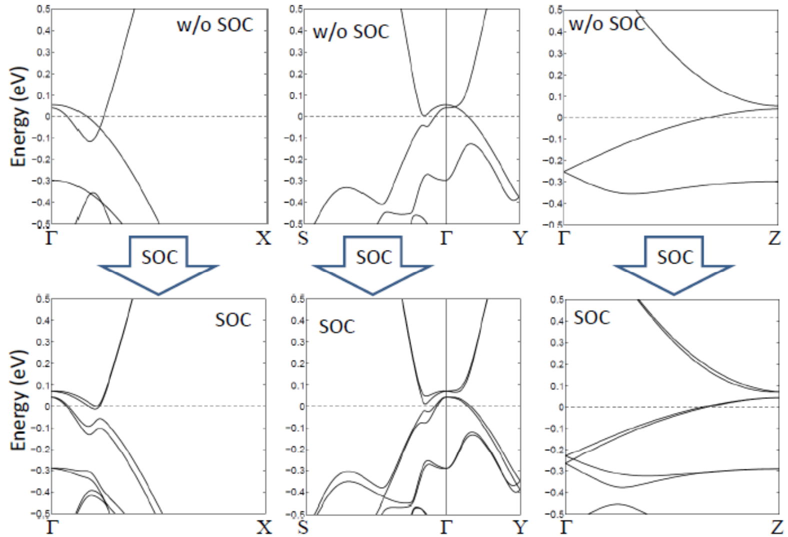


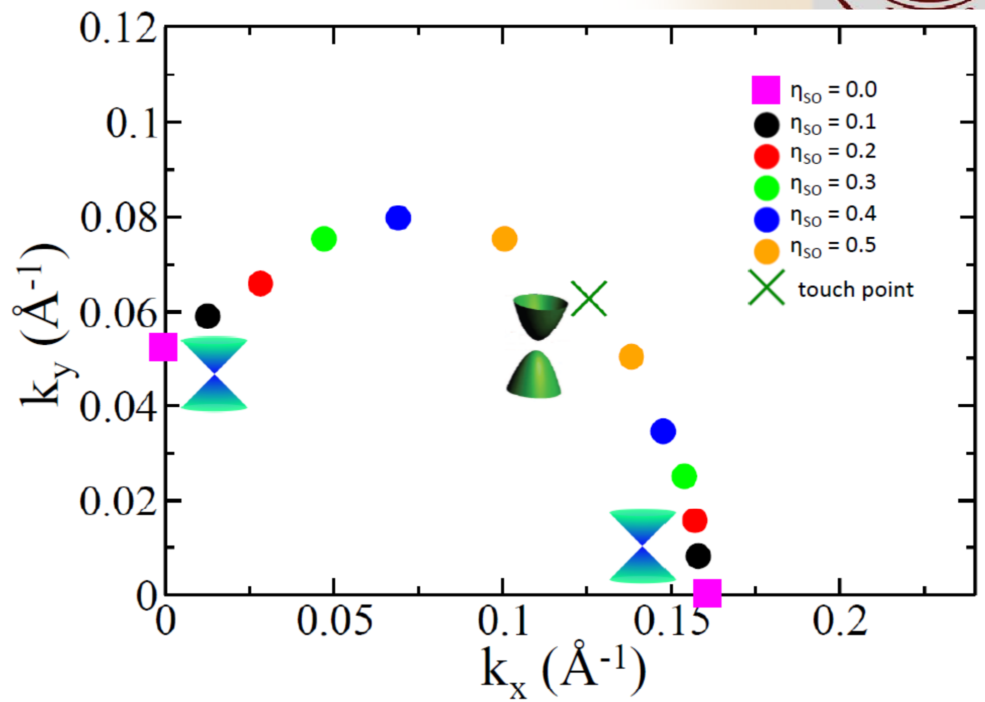


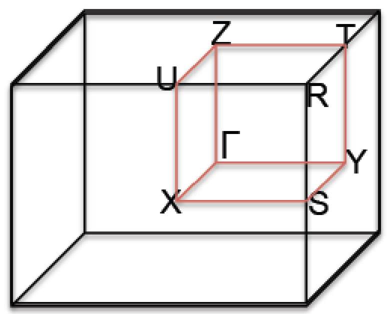


- 8 Weyl nodes born with small SOC
- Move in k-space with SOC increasing
- Annihilate at certain SOC

# Difficulty for Growing Single Crystals $\beta$-$Ag_2Se$

- High-T α-Phase: Super-Ionic, Cubic Im-3m, a~5 Å
- Low-T β-Phase: Non-central-symmetric Orthorhombic $P2_12_12_1$
- β-Phase: a~4 Å, b and c ~7 Å
- 1st Order Structural Phase Transition at 133 °C with Giant Volume Change

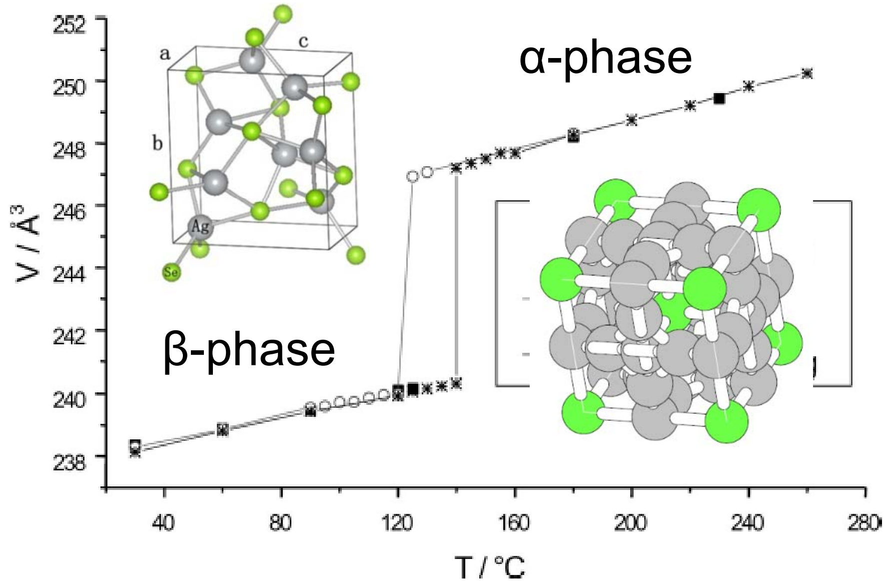


*H. Billetter and U. Ruschewitz* ***Z. Anorg. Allg. Chem****.* ***634:*** 241 (2008)

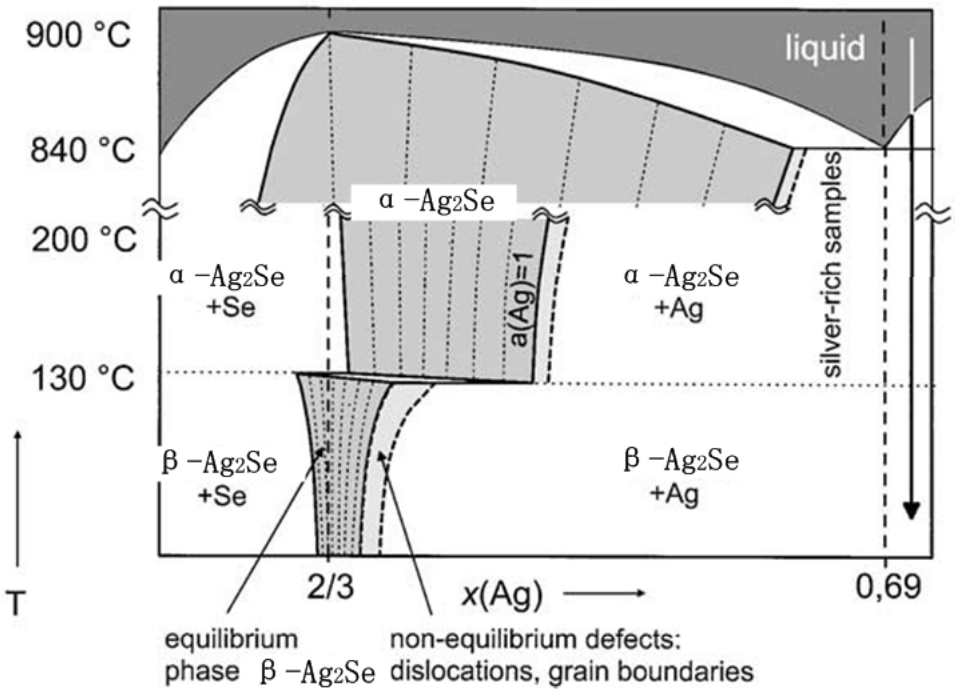


*G. Beck and J. Janek* ***Physica B 308-310:*** 1086 (2001)

***Bias : We cannot grow single crystals of such thermally unstable compound.***

# Single Crystal Growth: Vapor Transfer

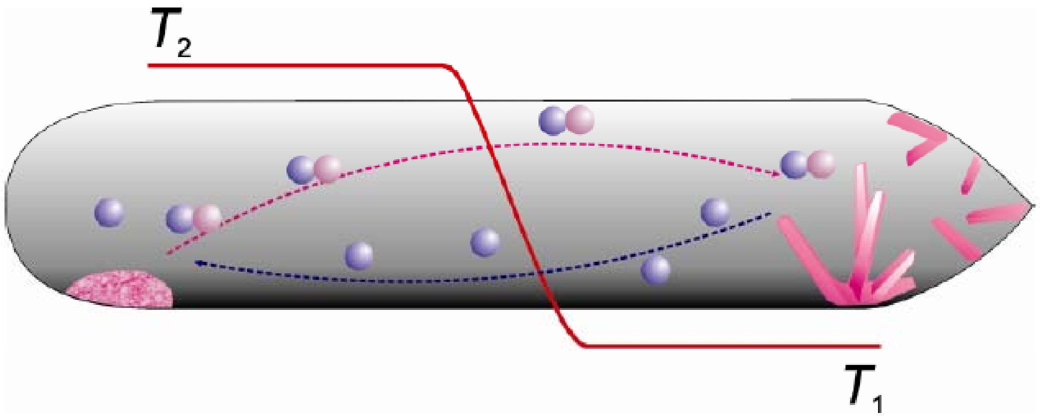


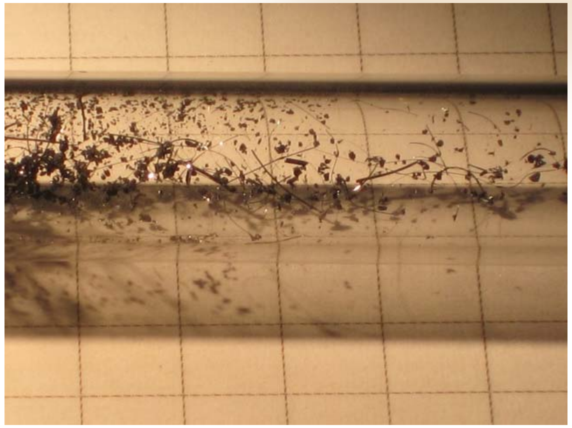

$Ag_2Se$ in a quartz tube

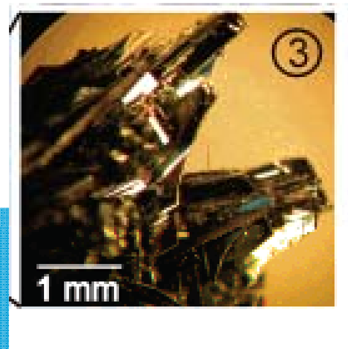


Black phosphorus via VT

- Forming crystals via gas phase
- Can be self-selected transfer or via agent
- Key point: agent, temperature, direction, “luck”
- Advantage: growing at low-T, clearer than flux-method, good for high-vapor-pressure elements

# Macro-size Single Crystals Synthesis of $Ag_2Se$

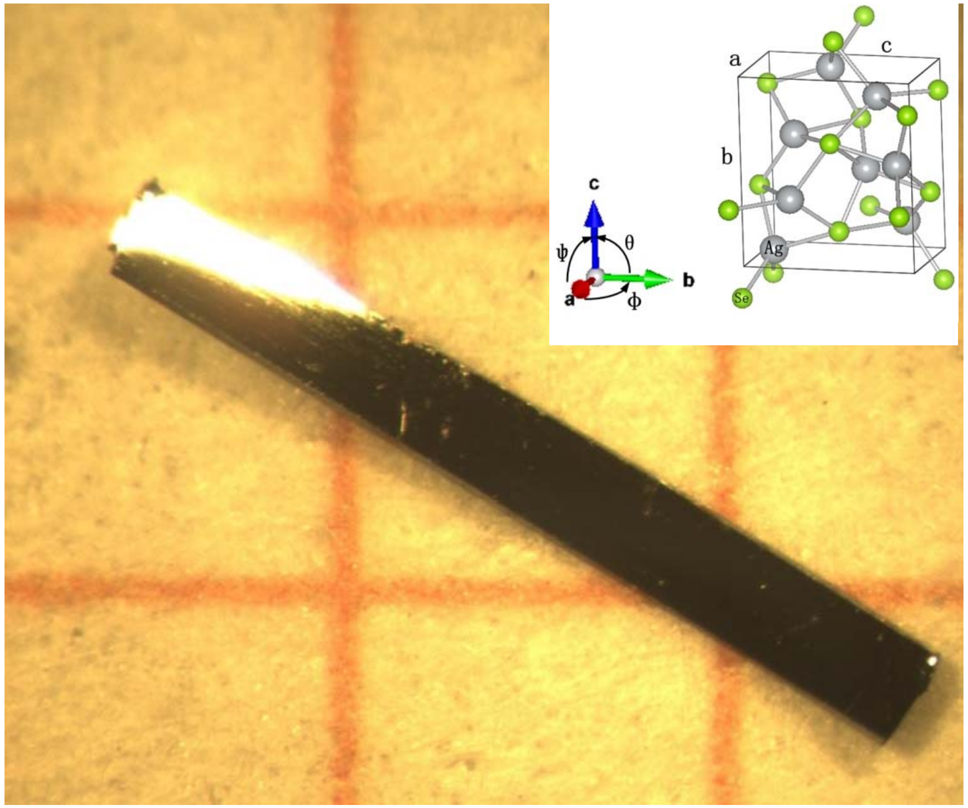


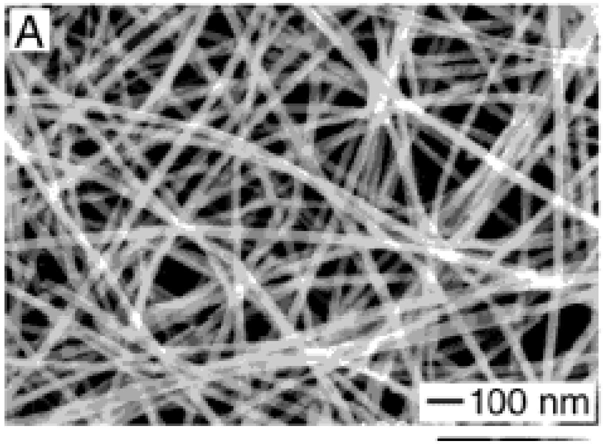


B. Gates *et. al.* ***JACS* 123:** 1150 (2001)

*For comparison, only nano-size crystals were synthesized before.*

- Crystals Grown Via Vapor Transfer Method
- Ribbon-Like Shape
- Size: up to 10 × 0.5 × 0.5 mm
- Confirmed by Single Crystal XRD

# Longitudinal MR: Strong SdH Oscillations +Negative LMR

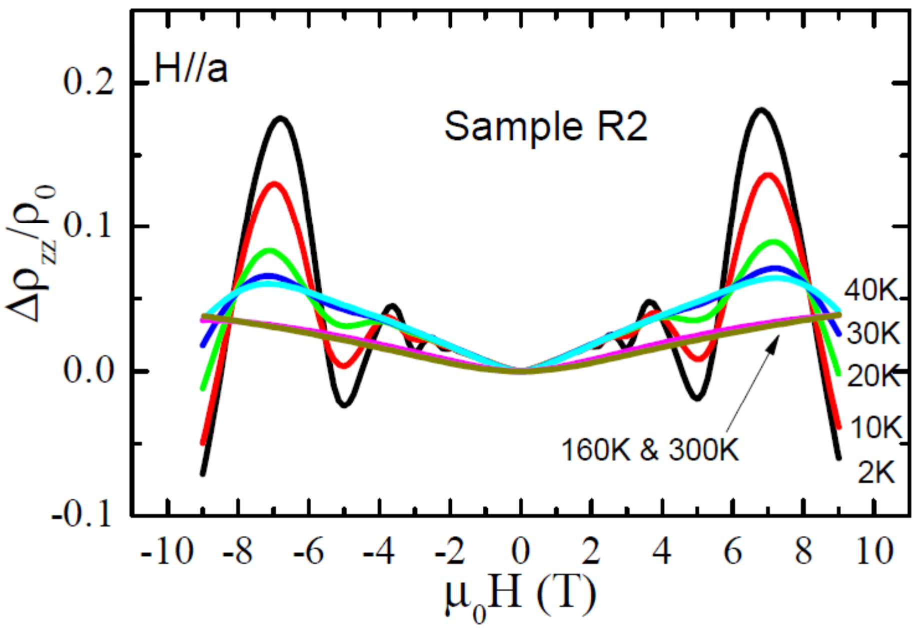


Large n

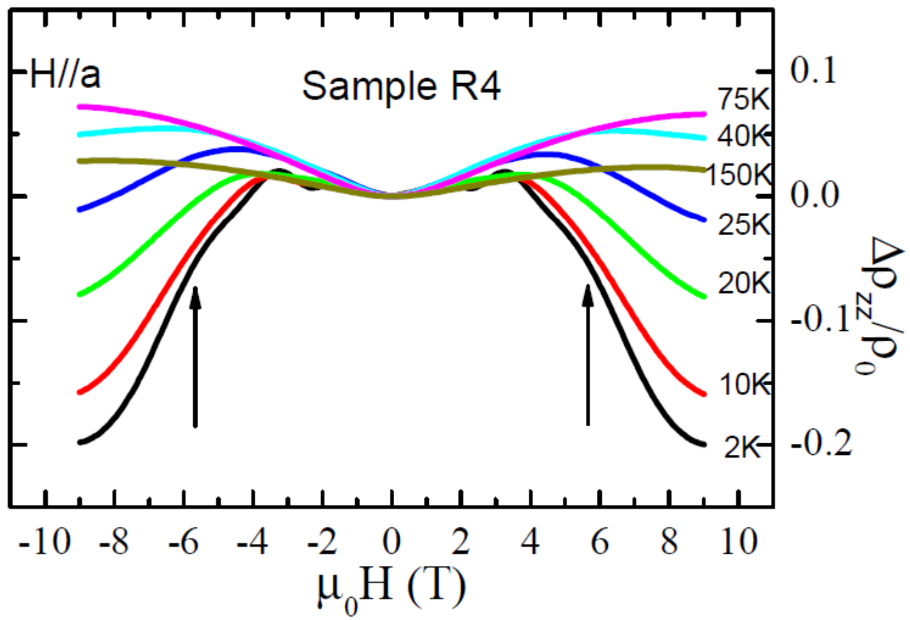


Small n

- Strong SdH Oscillations
- 1st Landau Level at 7T
- Negative LMR beyond 1st LL
- Oscillations and Negative LMR fade out when T ↑

- Relatively Weak Oscillations
- 1st LL at 3T
- Clear Negative LMR beyond 1st LL
- Anomaly at 6 T

# Highly Anisotropic Fermi Surface

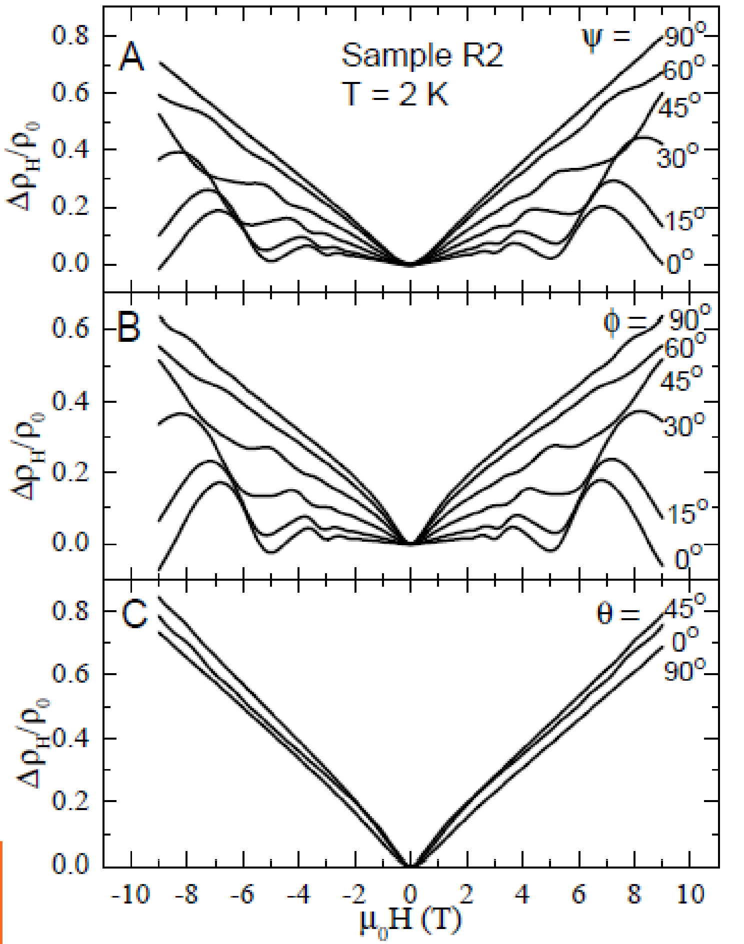


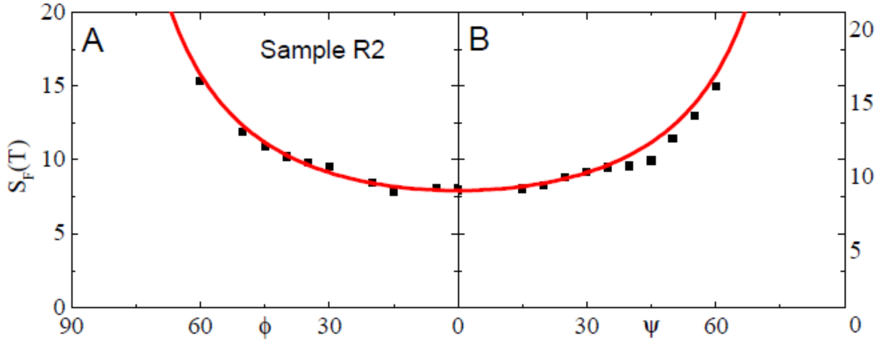


FS Follows $\frac{1}{cos\varphi}$ or $\frac{1}{cos\phi}$

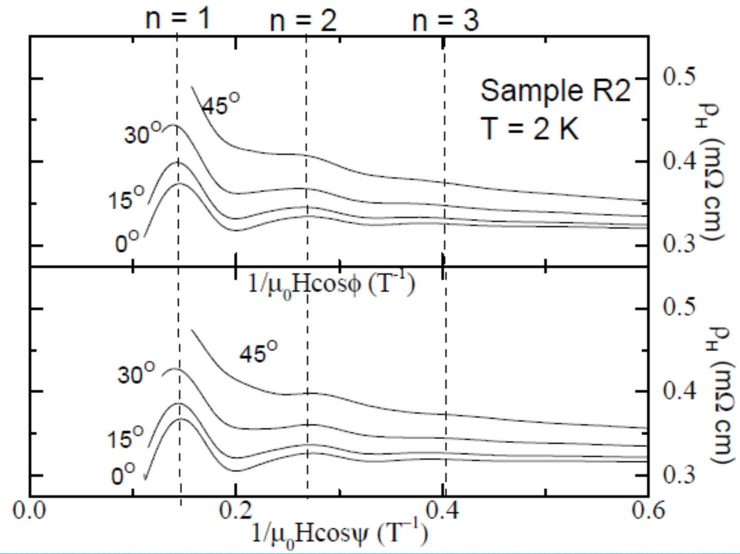



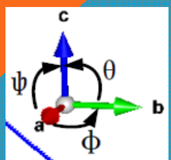


- MR from a to b/c are similar
- Invariant from b to c

FS : Cylinder or Highly Anisotropic Ellipsoid

# Dirac Fermions with Tiny Surface

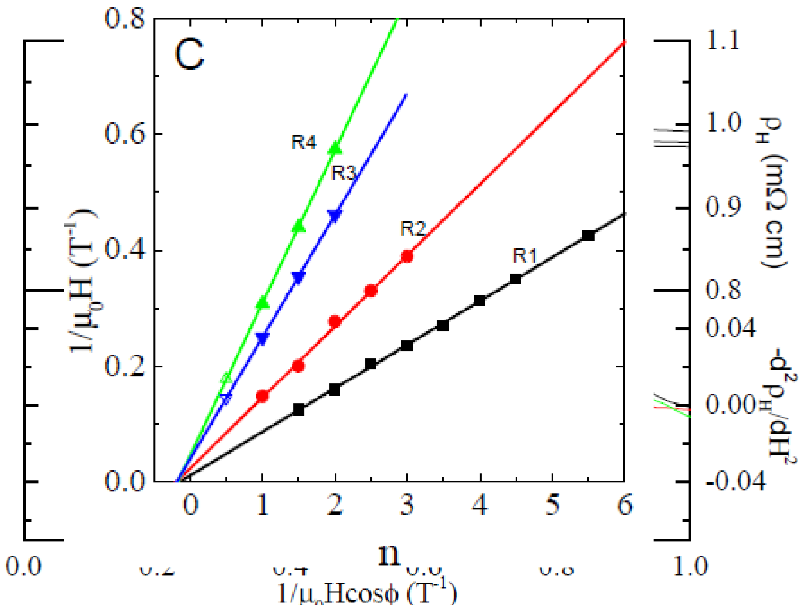


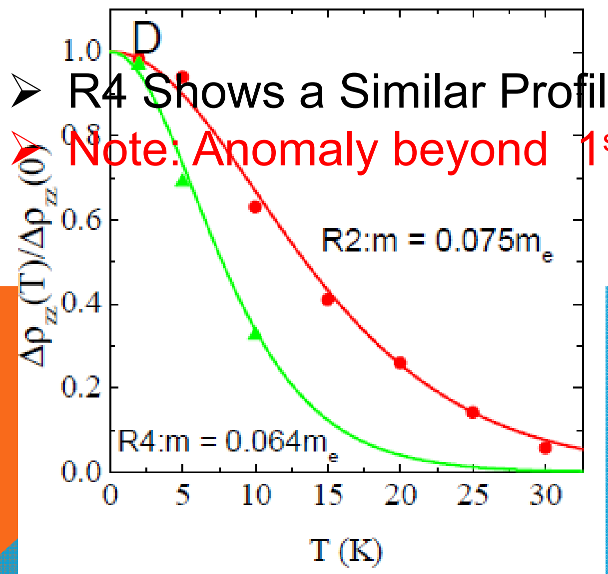


- R4 Shows a Similar Profile
- Note: Anomaly beyond 1st LL

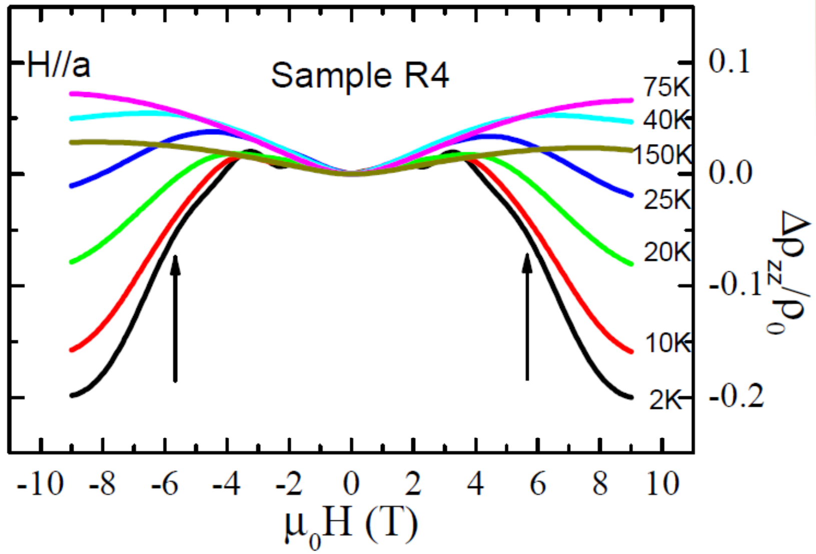


- FS: 13.3T~4T
- Onsager Phase $\gamma = -0.15 \pm 0.05$
- $m < 0.1m_e$
- $v_F \sim 2 \times 10^5 ms^{-1}$
- Consistent with a Linear Dispersive Band near Fermi Level
- The Anomaly at n = 1/2

# Negative LMR: Chiral Anomaly beyond QL

$P2_12_12_1$ Leads Symmetry Protected Weyl Nodes due to SOC

With no SOC

With SOC

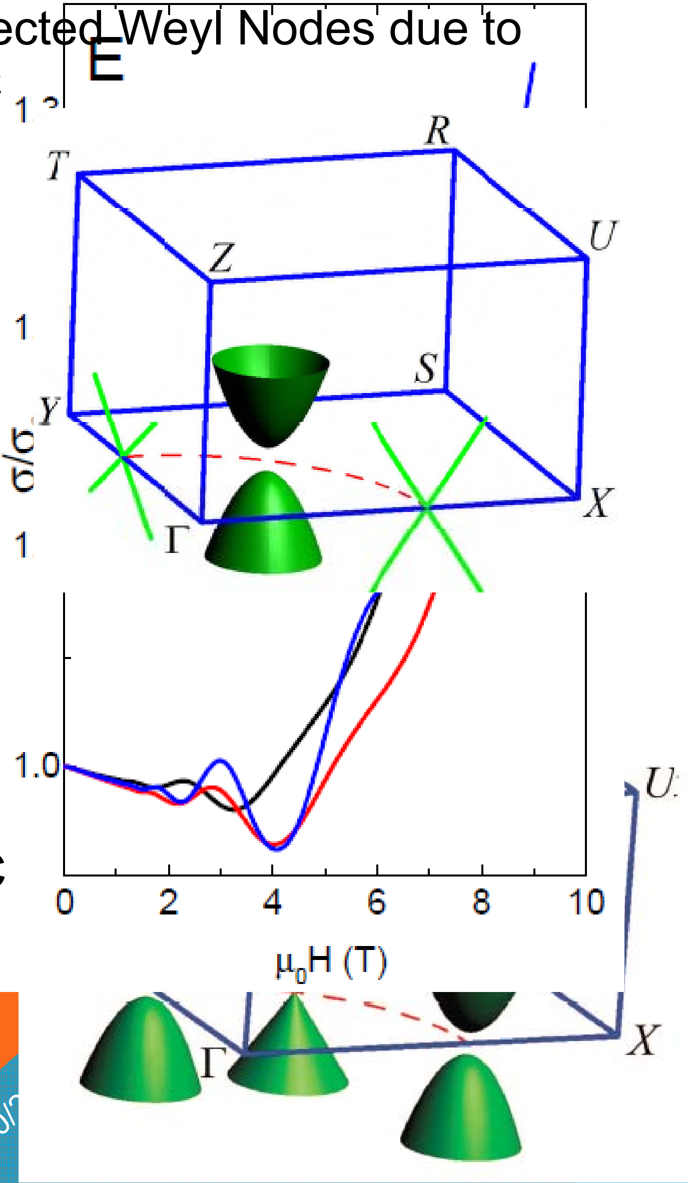


Charge Pumping Effect due to Chiral Anomaly beyond QL :

$$DOS \propto \vec{E}\cdot\vec{B} \propto \sigma$$

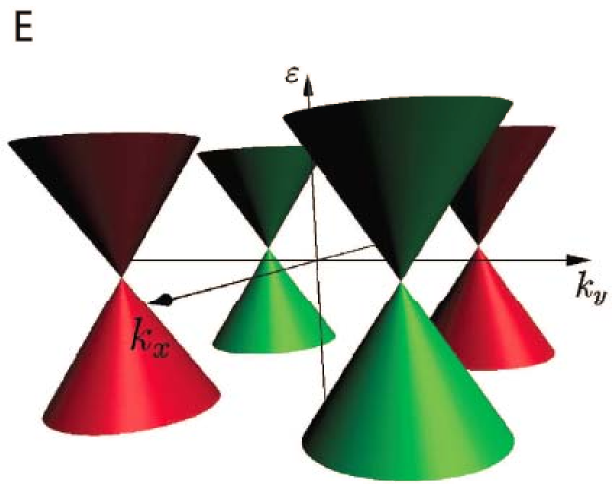


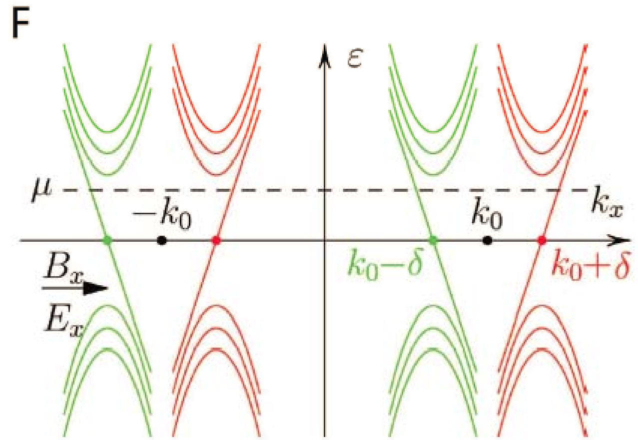

# TaAs: a Semimetal with Non-central Symmetric Structure

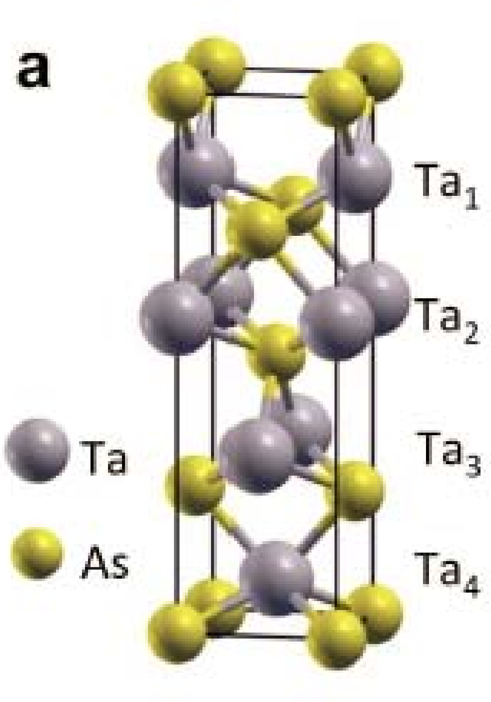


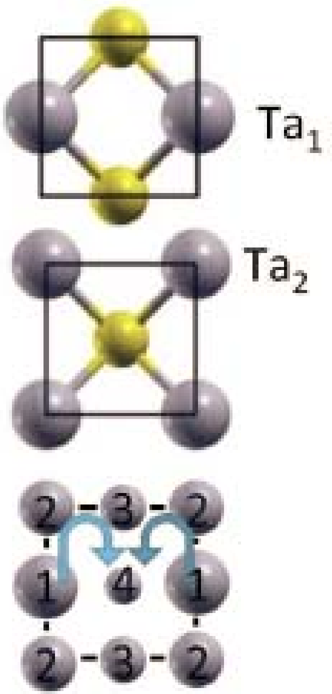


*Electric properties of polycrystals are not noteworthy*

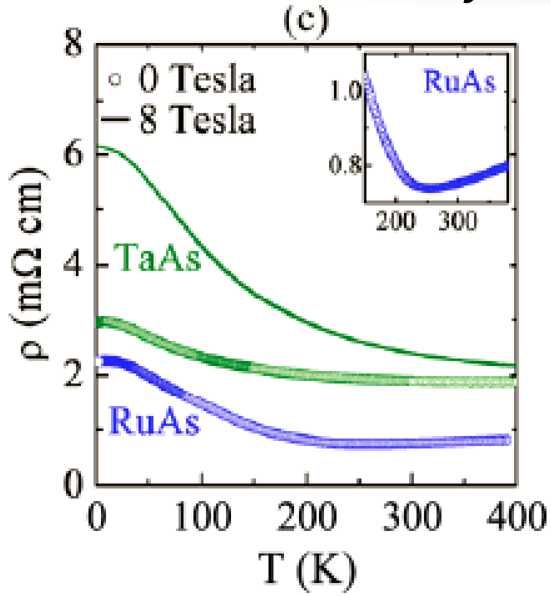


B. Saparov *etal*. 2012

- One Ta atom in a 6-atom As prism
- Space group: $I4_1md$
- Previous study on polycrystals show semiconductor/semimetal behaviors
- Single crystals grown via vapor transfer method

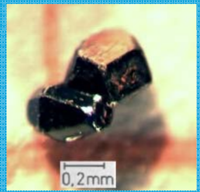

# TaAs, NbAs, TaP and NbP: Relatively Structure in Pnictides

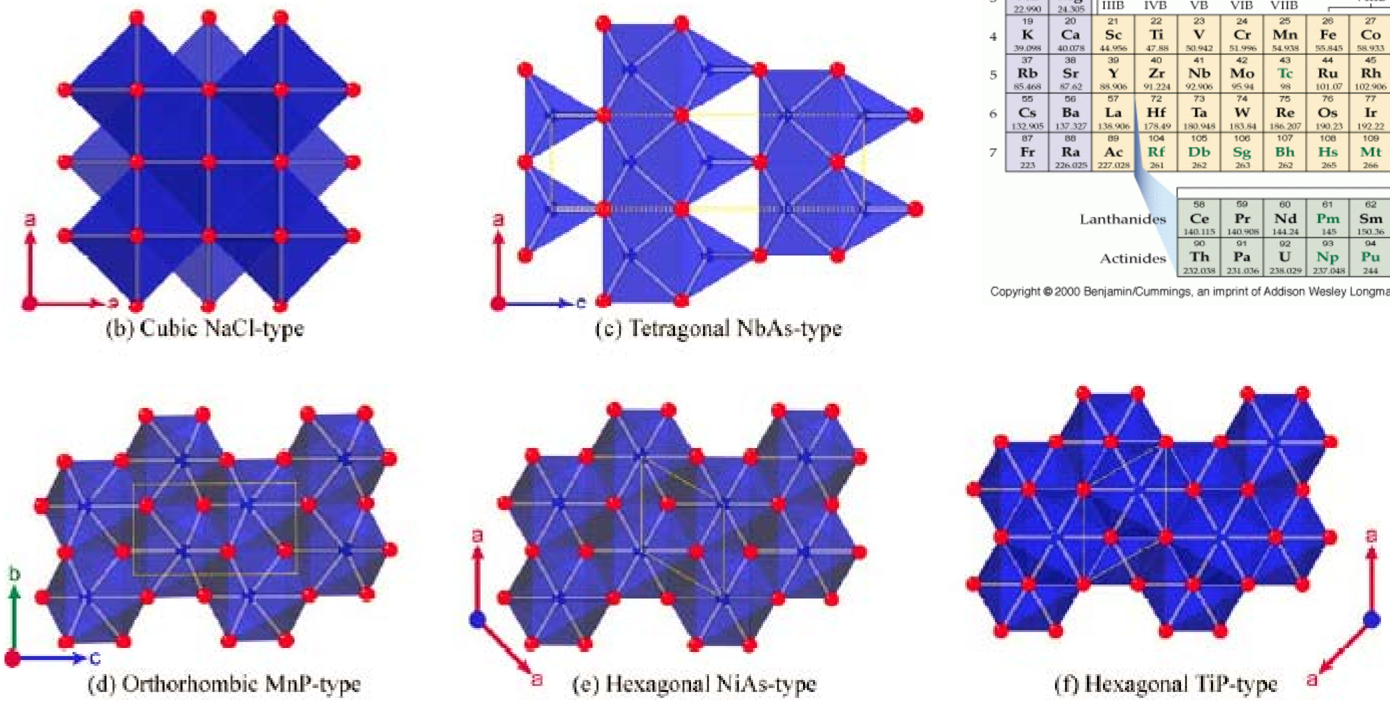

(b) Cubic NaCl-type (c) Tetragonal NbAs-type

(d) Orthorhombic MnP-type (e) Hexagonal NiAs-type (f) Hexagonal TiP-type

**Periodic Table of the Elements**

Representative (main group) elements — Transition metals — Representative (main group) elements

| | IA | IIA | IIIB | IVB | VB | VIB | VIIB | VIIIB | VIIIB | VIIIB | IB | IIB | IIIA | IVA | VA | VIA | VIIA | VIIIA |
|---|---|---|---|---|---|---|---|---|---|---|---|---|---|---|---|---|---|---|
| 1 | 1 H 1.0079 | | | | | | | | | | | | | | | | | 2 He 4.003 |
| 2 | 3 Li 6.941 | 4 Be 9.012 | | | | | | | | | | | 5 B 10.811 | 6 C 12.011 | 7 N 14.007 | 8 O 15.999 | 9 F 18.998 | 10 Ne 20.180 |
| 3 | 11 Na 22.990 | 12 Mg 24.305 | | | | | | | | | | | 13 Al 26.982 | 14 Si 28.086 | 15 P 30.974 | 16 S 32.066 | 17 Cl 35.453 | 18 Ar 39.948 |
| 4 | 19 K 39.098 | 20 Ca 40.078 | 21 Sc 44.956 | 22 Ti 47.88 | 23 V 50.942 | 24 Cr 51.996 | 25 Mn 54.938 | 26 Fe 55.845 | 27 Co 58.933 | 28 Ni 58.69 | 29 Cu 63.546 | 30 Zn 65.39 | 31 Ga 69.723 | 32 Ge 72.61 | 33 As 74.922 | 34 Se 78.96 | 35 Br 79.904 | 36 Kr 83.8 |
| 5 | 37 Rb 85.468 | 38 Sr 87.62 | 39 Y 88.906 | 40 Zr 91.224 | 41 Nb 92.906 | 42 Mo 95.94 | 43 Tc 98 | 44 Ru 101.07 | 45 Rh 102.906 | 46 Pd 106.42 | 47 Ag 107.868 | 48 Cd 112.411 | 49 In 114.82 | 50 Sn 118.71 | 51 Sb 121.76 | 52 Te 127.60 | 53 I 126.905 | 54 Xe 131.29 |
| 6 | 55 Cs 132.905 | 56 Ba 137.327 | 57 La 138.906 | 72 Hf 178.49 | 73 Ta 180.948 | 74 W 183.84 | 75 Re 186.207 | 76 Os 190.23 | 77 Ir 192.22 | 78 Pt 195.08 | 79 Au 196.967 | 80 Hg 200.59 | 81 Tl 204.383 | 82 Pb 207.2 | 83 Bi 208.980 | 84 Po 209 | 85 At 210 | 86 Rn 222 |
| 7 | 87 Fr 223 | 88 Ra 226.025 | 89 Ac 227.028 | 104 Rf 261 | 105 Db 262 | 106 Sg 263 | 107 Bh 262 | 108 Hs 265 | 109 Mt 266 | 110 Uun 269 | 111 Uuu 272 | 112 Uub 277 | | 114 | | 116 | | 118 |

Rare earth elements

| | | | | | | | | | | | | | | |
|---|---|---|---|---|---|---|---|---|---|---|---|---|---|---|
| Lanthanides | 58 Ce 140.115 | 59 Pr 140.908 | 60 Nd 144.24 | 61 Pm 145 | 62 Sm 150.36 | 63 Eu 151.964 | 64 Gd 157.25 | 65 Tb 158.925 | 66 Dy 162.5 | 67 Ho 164.93 | 68 Er 167.26 | 69 Tm 168.934 | 70 Yb 173.04 | 71 Lu 174.967 |
| Actinides | 90 Th 232.038 | 91 Pa 231.036 | 92 U 238.029 | 93 Np 237.048 | 94 Pu 244 | 95 Am 243 | 96 Cm 247 | 97 Bk 247 | 98 Cf 251 | 99 Es 252 | 100 Fm 257 | 101 Md 258 | 102 No 259 | 103 Lr 262 |

# Band Structure of TaAs

With no SOC: band touching

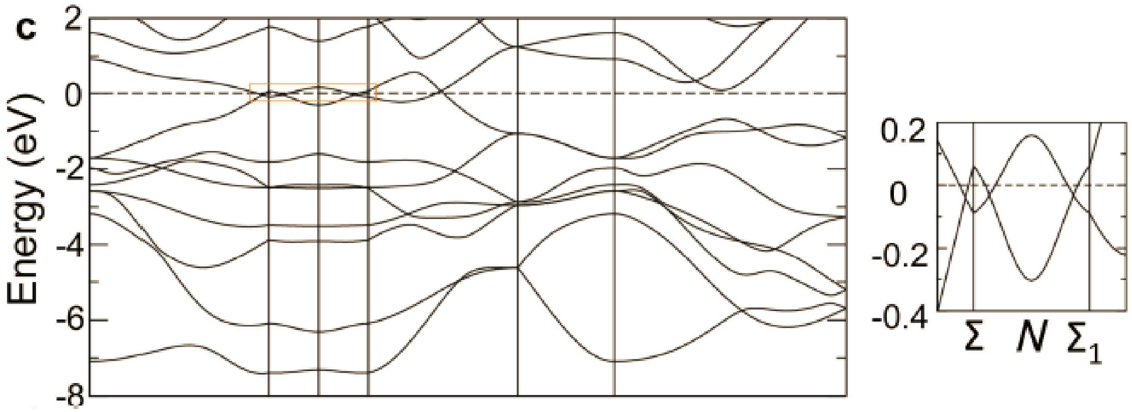


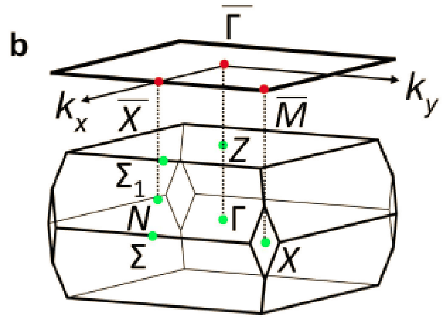


The BZ of TaAs

With SOC: open a small gap in high symmetric lines

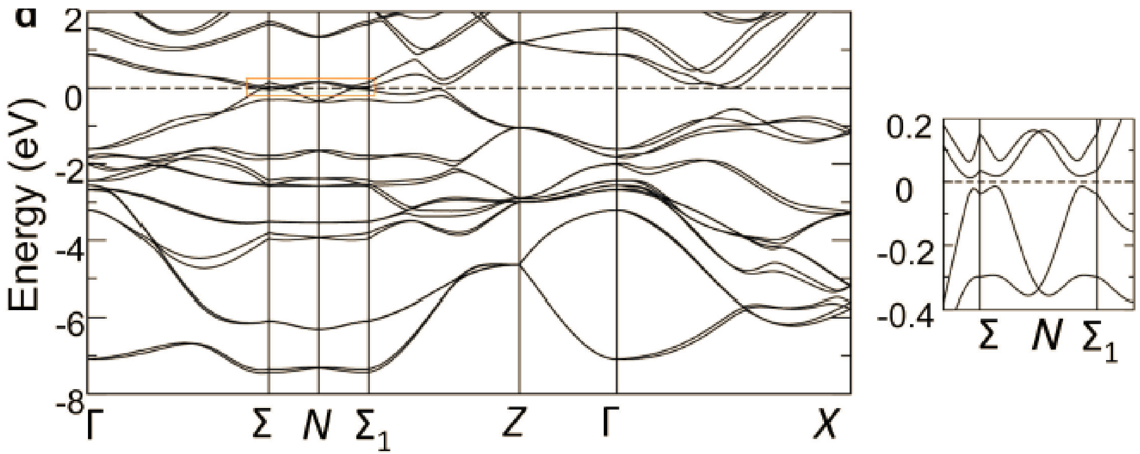


S. Huang *etal.* Arxiv:1501.00755(2015)
Similar results in H. Weng *etal.* PRX 5 011029 (2015)

# Weyl Nodes in TaAs (calculated)

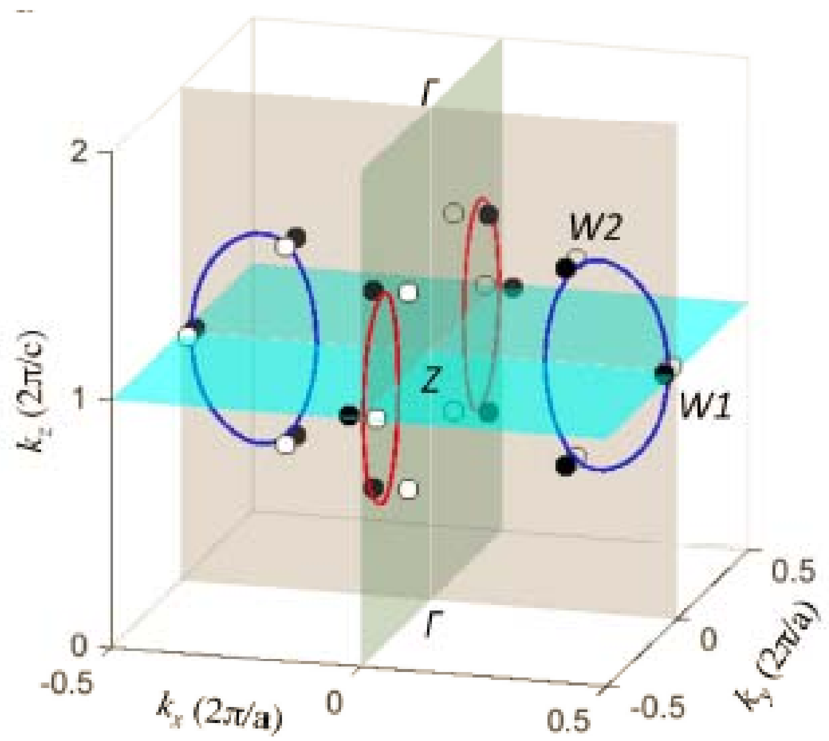


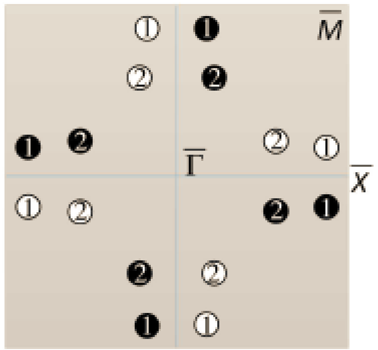


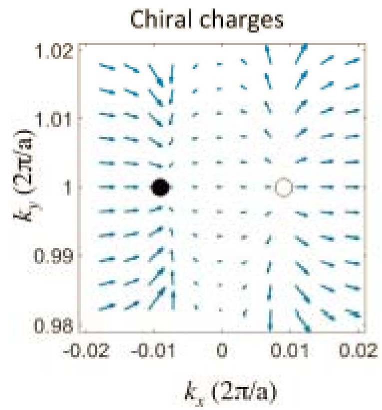


- Each line node vaporizes into six Weyl points
- 8 W1 on one plane, 16 W2 away from the plane
- Spin texture shows opposite chirality

S. Huang *etal.* Arxiv:1501.00755(2015)
Similar results in H. Weng *etal.* PRX 5 011029 (2015)

# Surface Fermi Arc in TaAs

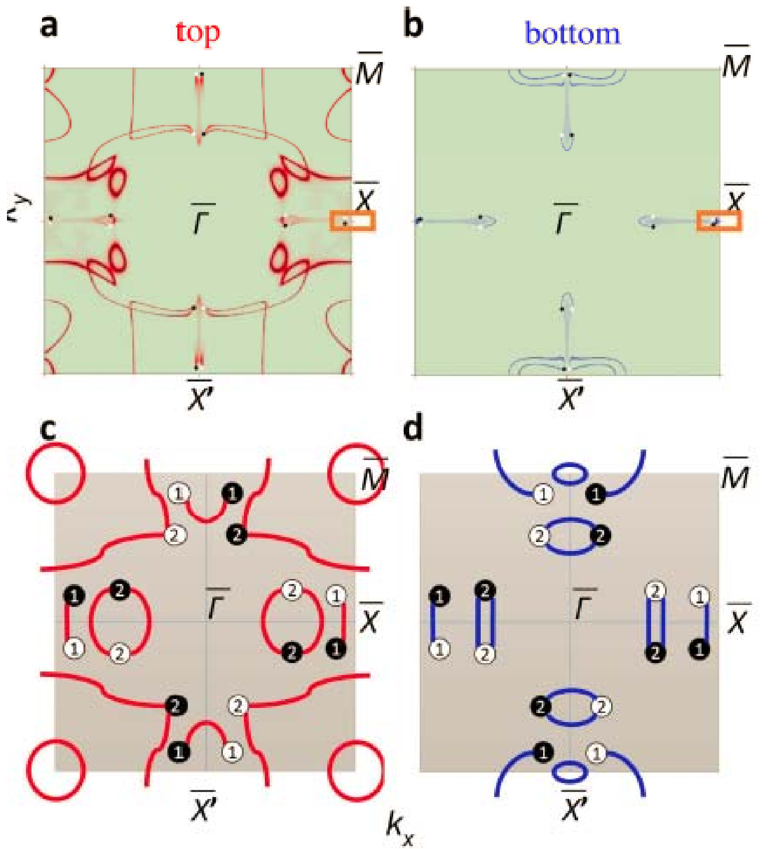


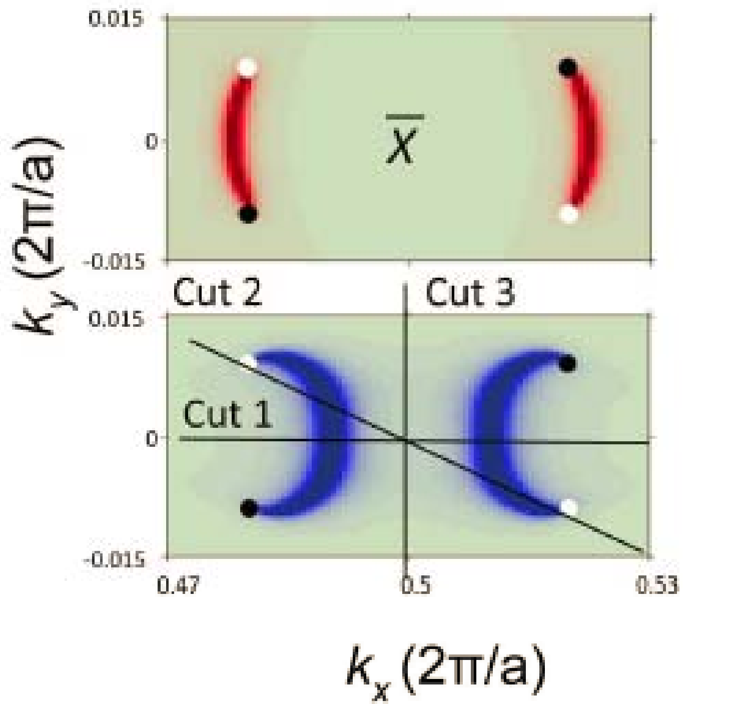


The (001) surface states on the top and bottom surface of TaAs

A close-up of the Fermi arc on the surface

S. Huang *etal.* Arxiv:1501.00755(2015)
Similar results in H. Weng *etal.* PRX 5 011029 (2015)

# ARPES: Observing the Surface Fermi Arc and Weyl Nodes in Experiment

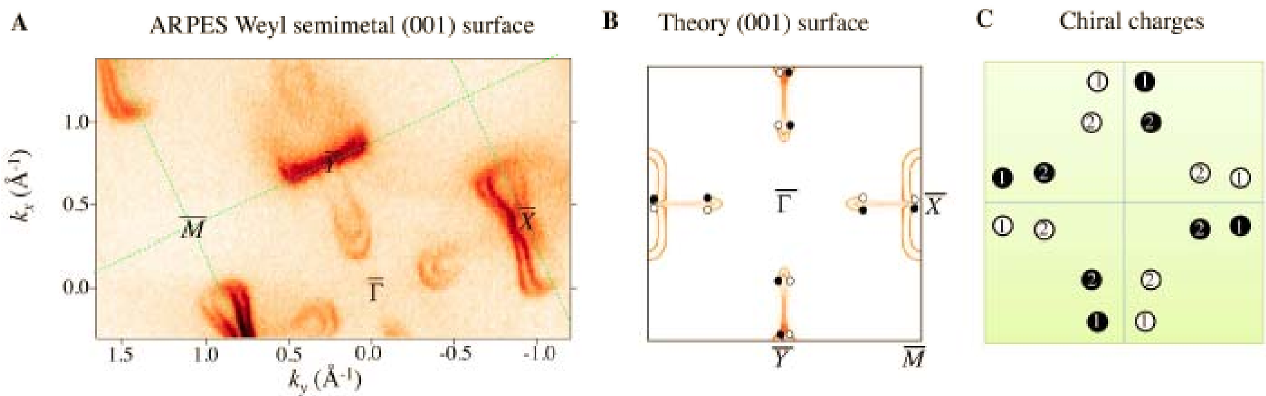


Observed Fermi Arc surface states

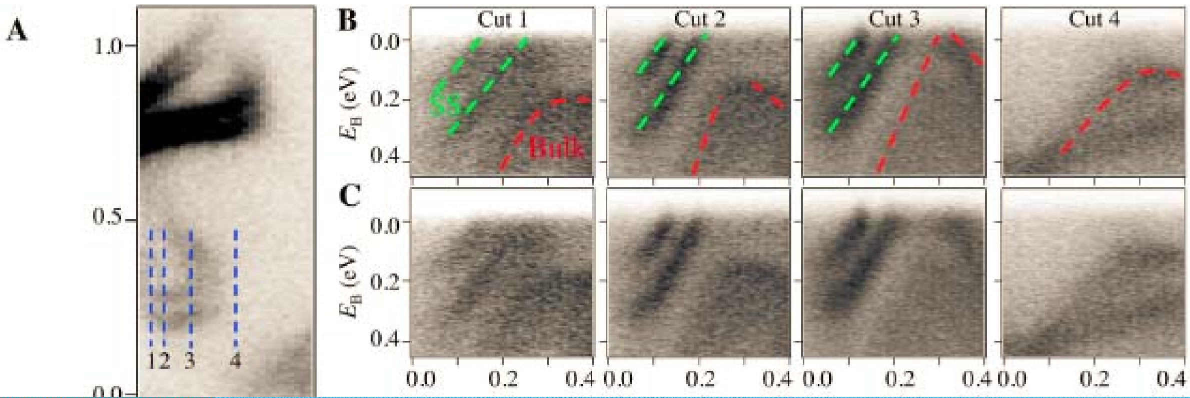


The Weyl cone rises up to meet the Fermi arcs

SY Xu *etal.* Arxiv:1501.03807(2015)
Similar results in B.Q Lv *etal.* Arxiv: 1502.04684(2015)

# Observation of Clear Weyl Nodes and Fermi Arcs in NbAs

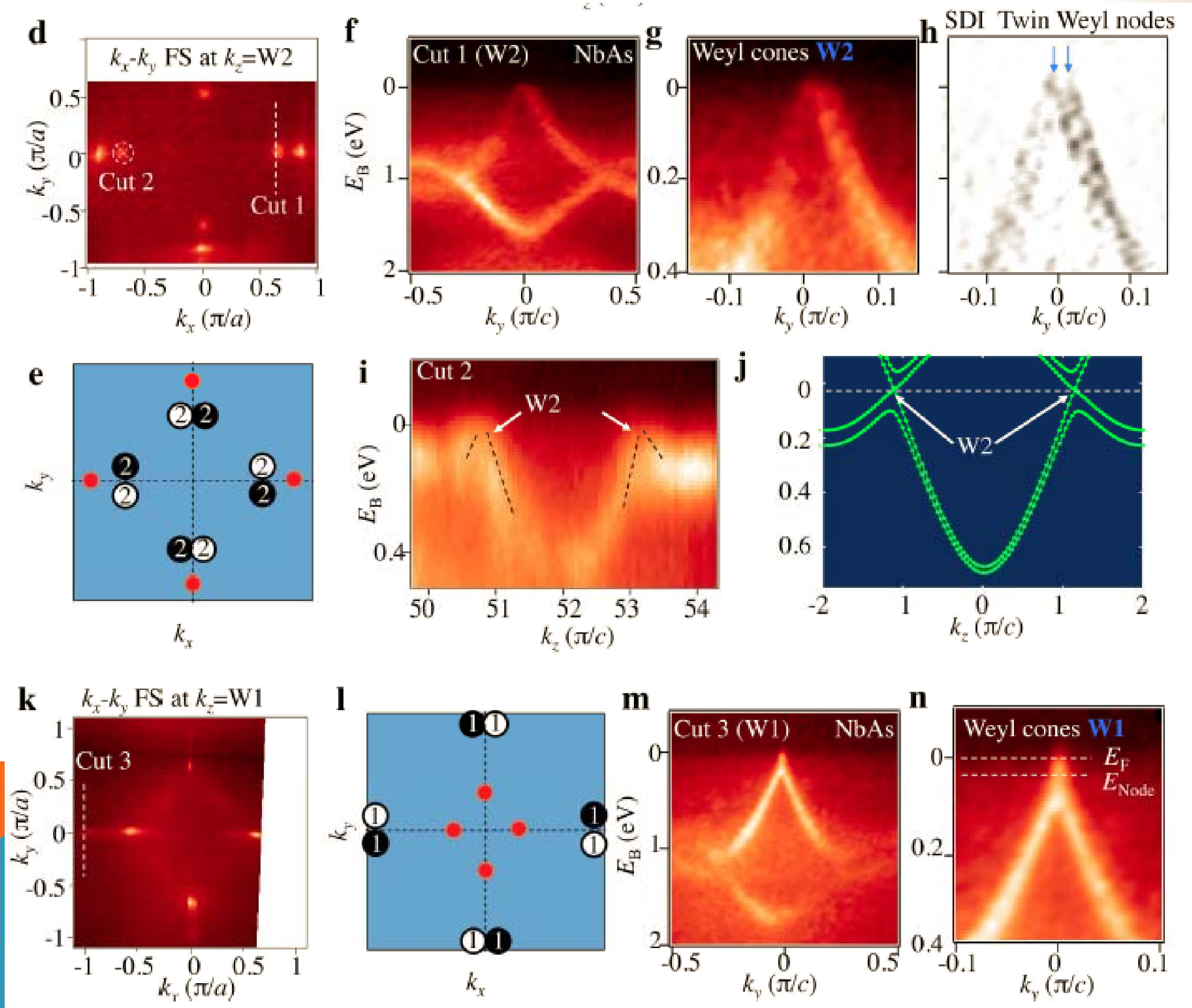




More details in Su-yang Xu *etal*. arXiv:1504.01350

# Transport Property: Large MR in TaAs

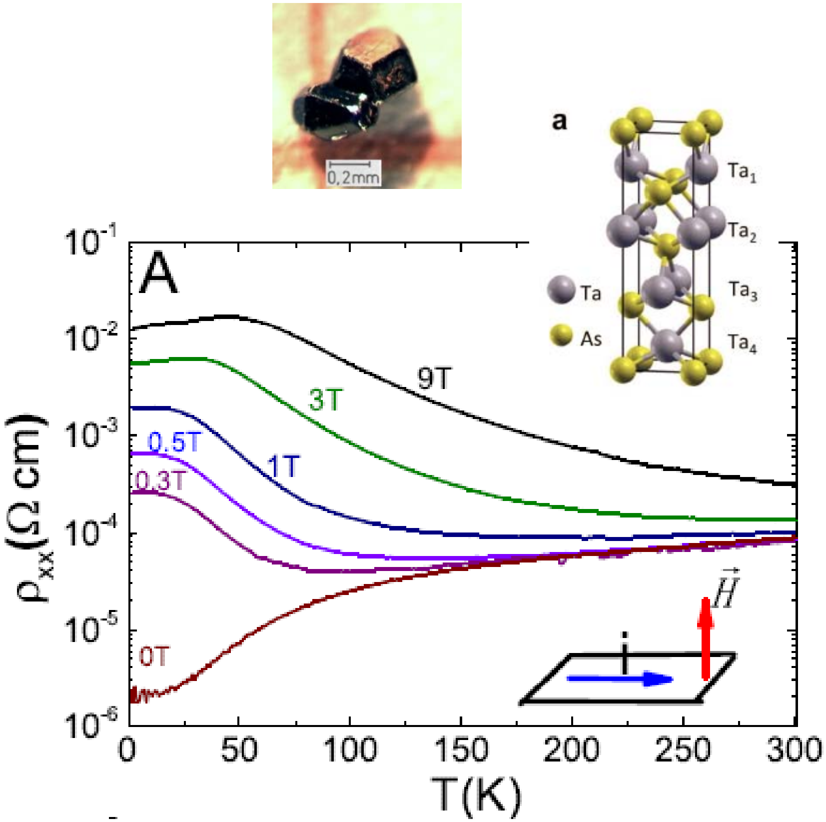


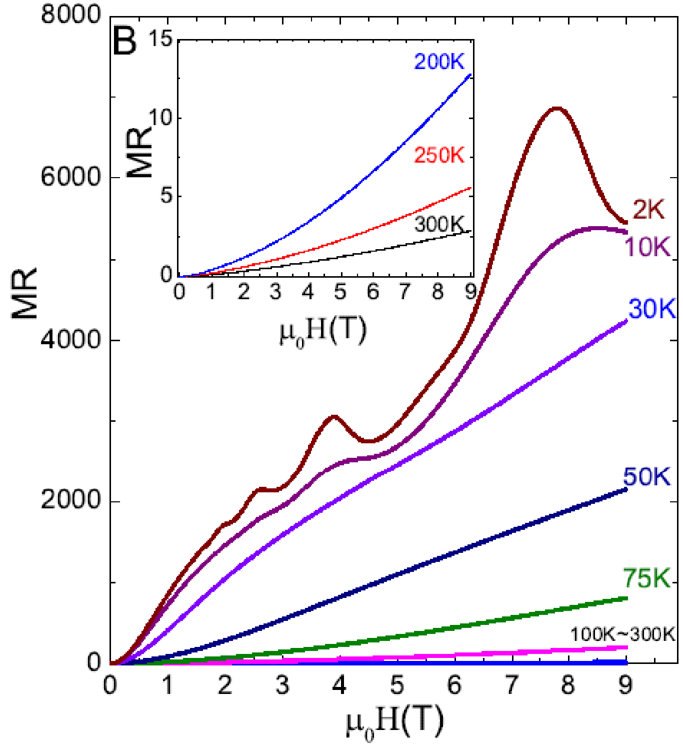


- A small field turns on TaAs to be an insulator
- In 9T, MR~5000 at 2K and ~3 at 300K (MR = $\rho_H/\rho_0$-1 )
- Extremely strong SdH oscillations at low T

# Linear MR with Strong SdH Oscillations at Low T

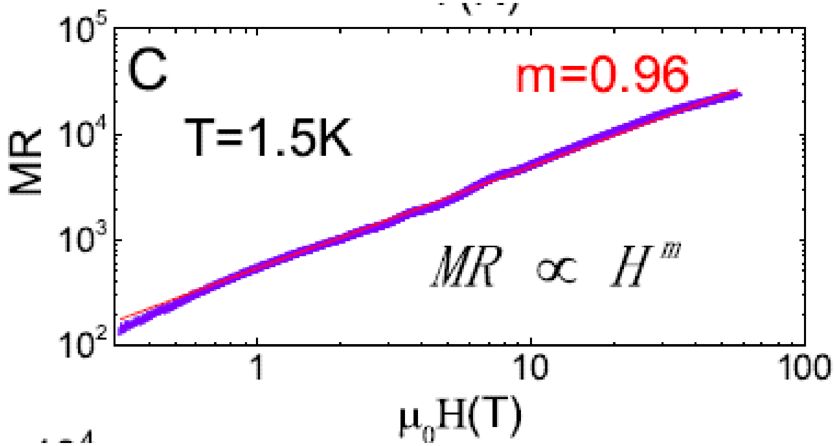


A linear MR beyond the QL up to 55T at low T

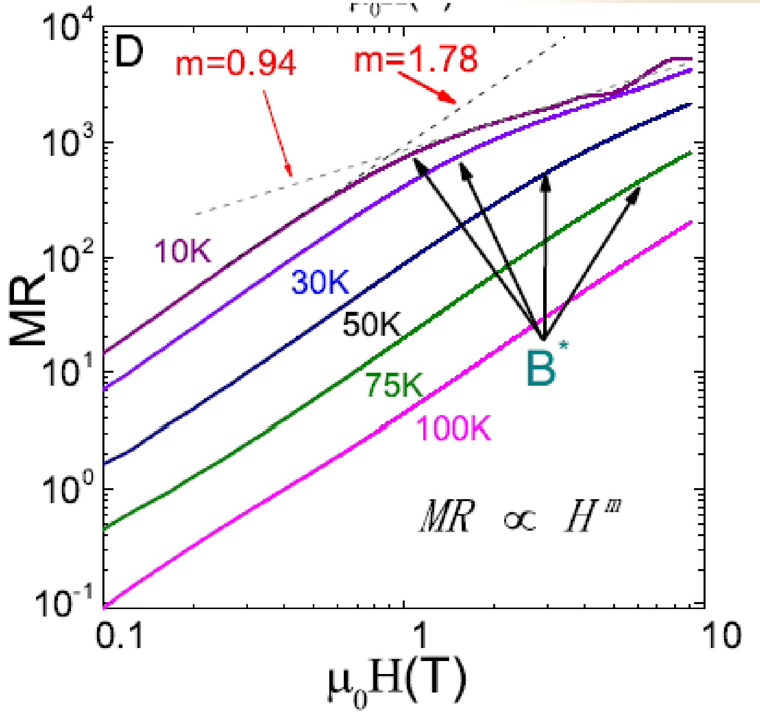


MR changes from parabolic to linear at certain B

# Two-band Features in Hall Resistance

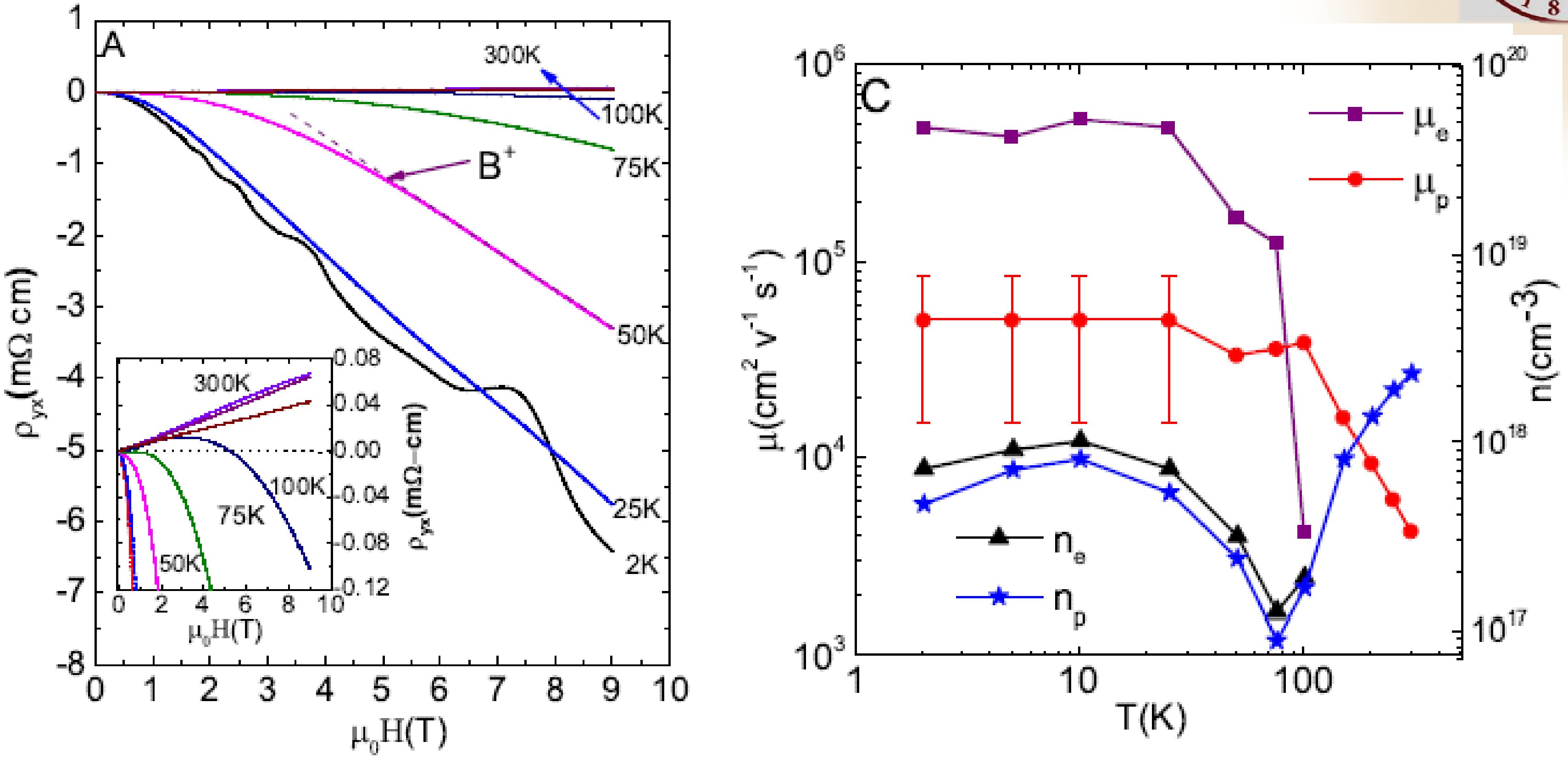


- Compensated semimetal with n and p ~$10^{17}$cm$^{-3}$
- e channel with much higher mobility opens below 100K
- Low T features are dominated by e channel

# Quantum Oscillations in $\rho_{xx}$ and $\rho_{xy}$

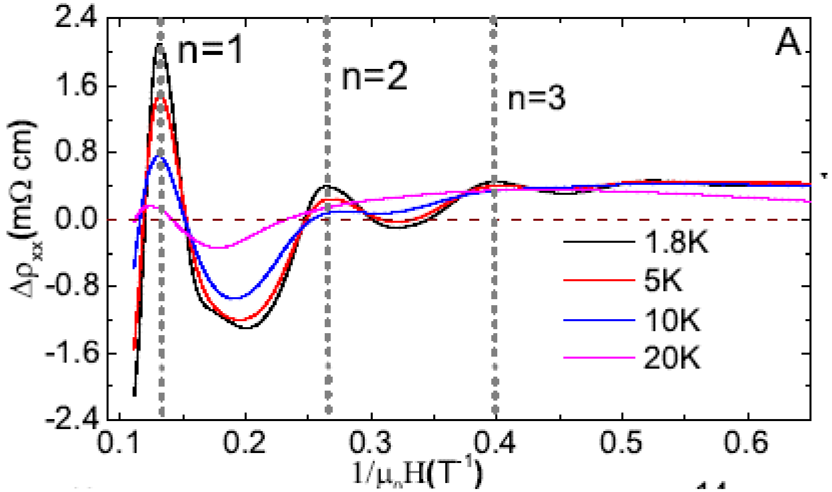


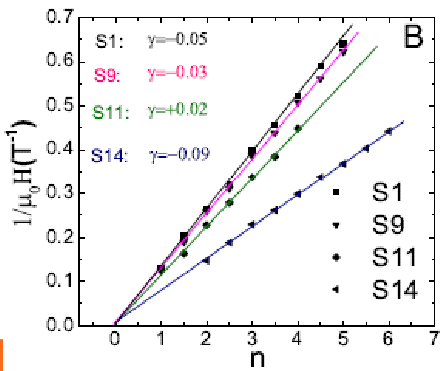


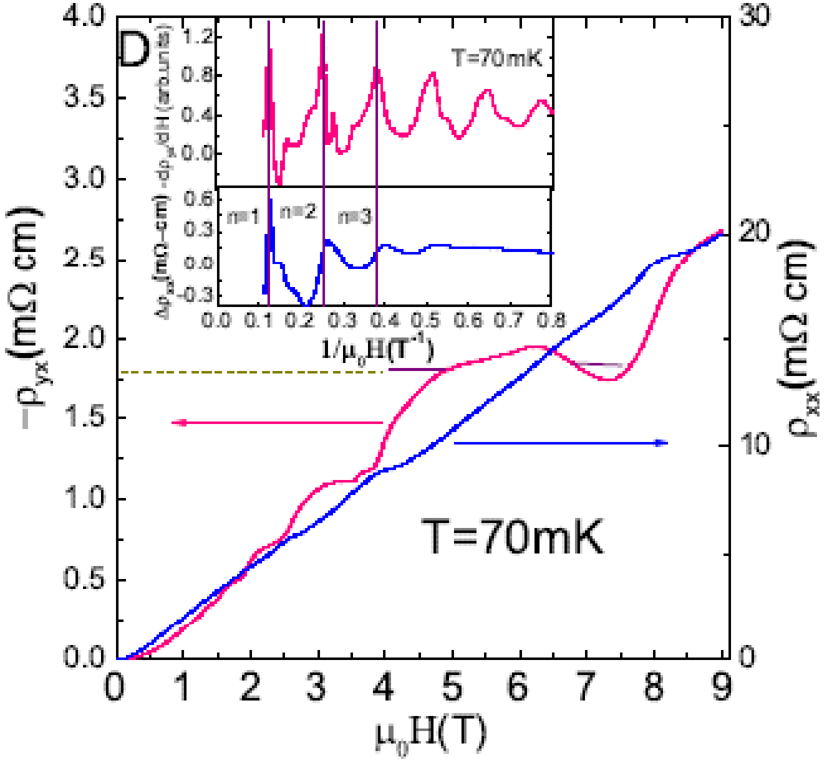


- Strong oscillations come from a tiny e pocket ~ 8T
- Non-trivial Berry phase

More interesting features at low-T

# Fermi Surface Topology from Transport

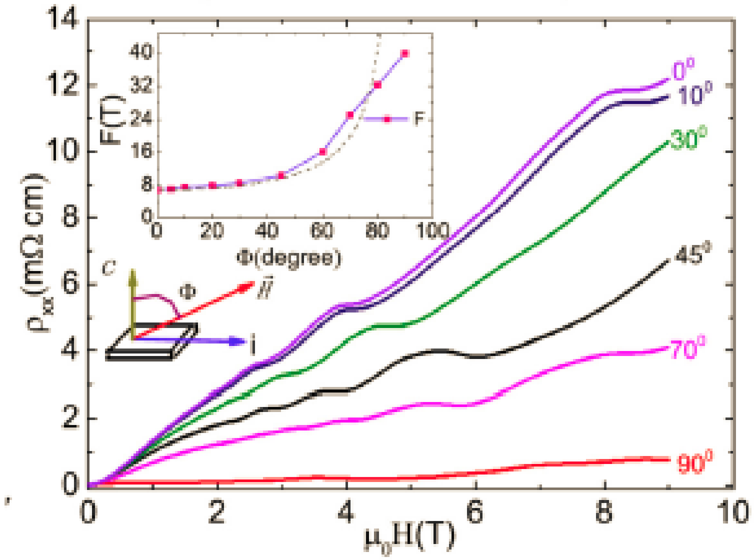


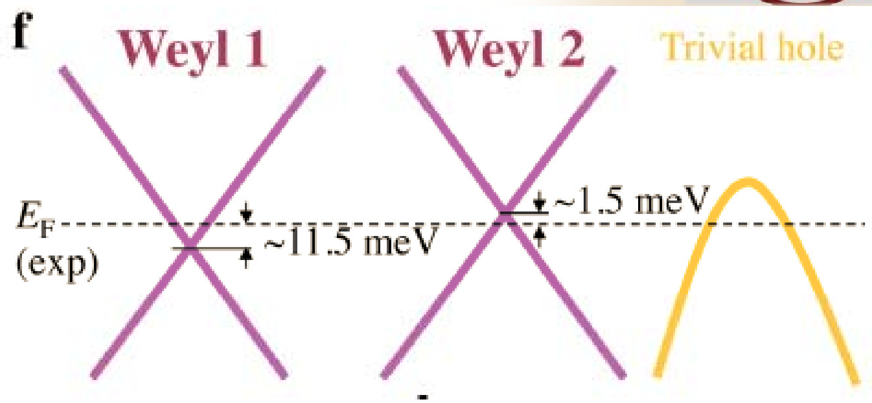


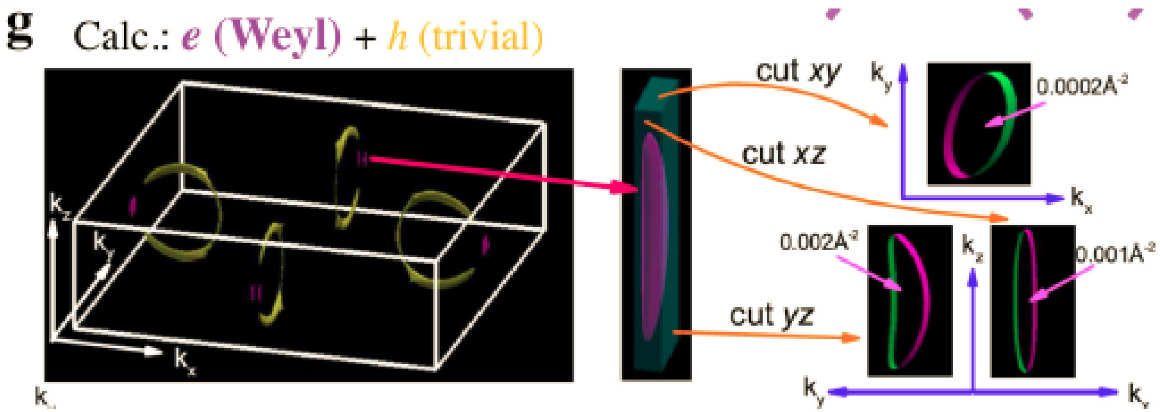


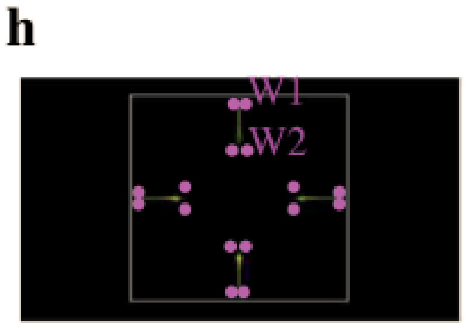


- An ellipsoid-like shape FS consistent with calculations
- Fermi level crosses two Weyl cones and one trivial hole band

# Chiral Anomaly

Low field σ is expressed as $\sigma(H) = \left(\sigma_0 + a\sqrt{H}\right)\left(1 + C_W H^2\right) + \frac{1}{\rho + A H^2} + \frac{1}{\rho' + A' H^2},$

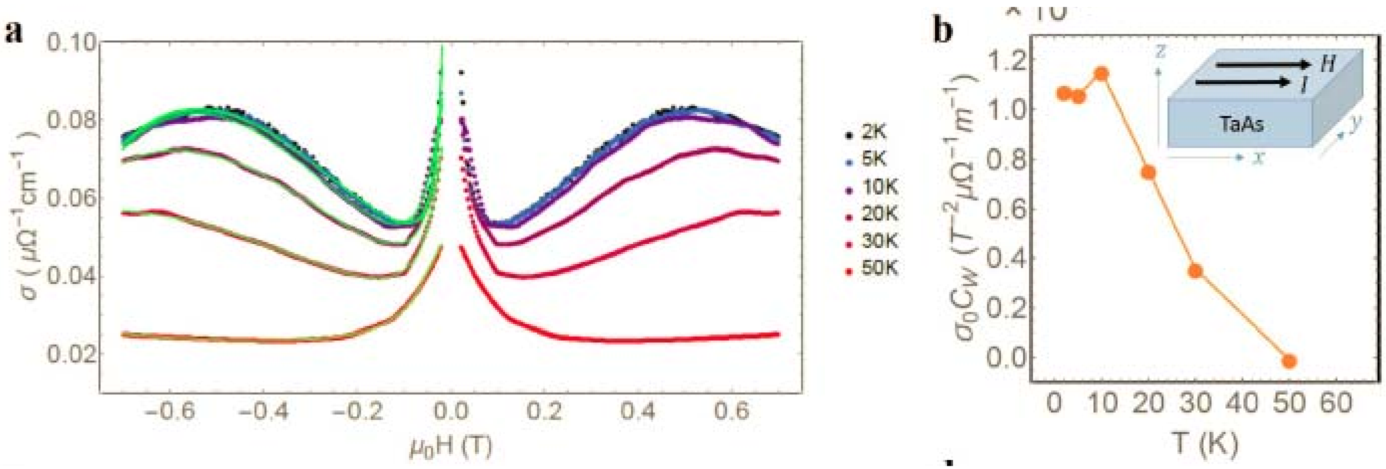


T dependent chiral anomaly contribution

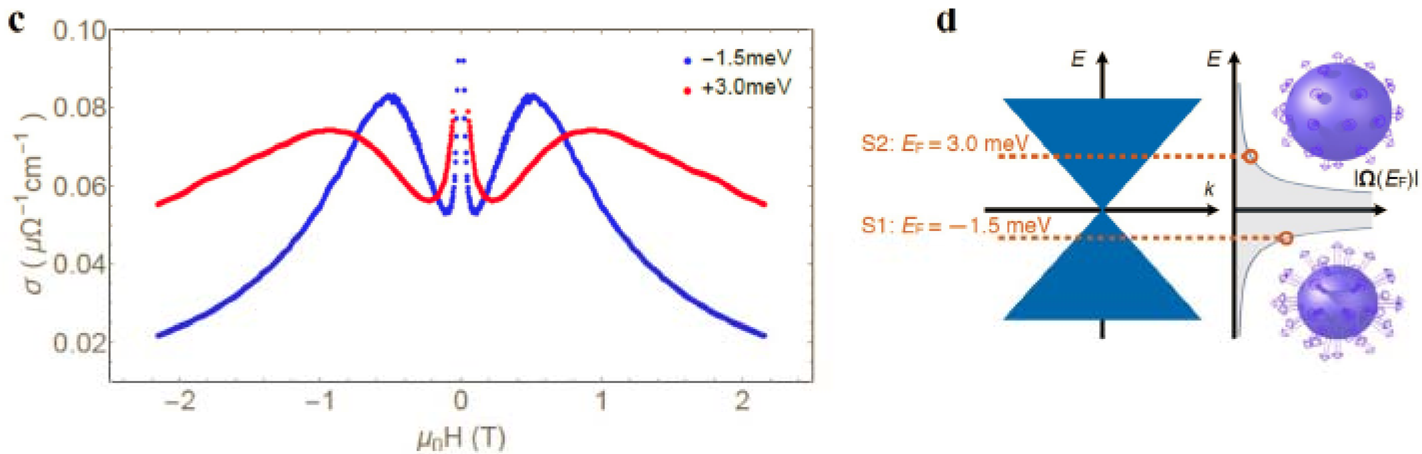


Different samples with different Fermi level

# Chiral Anomaly

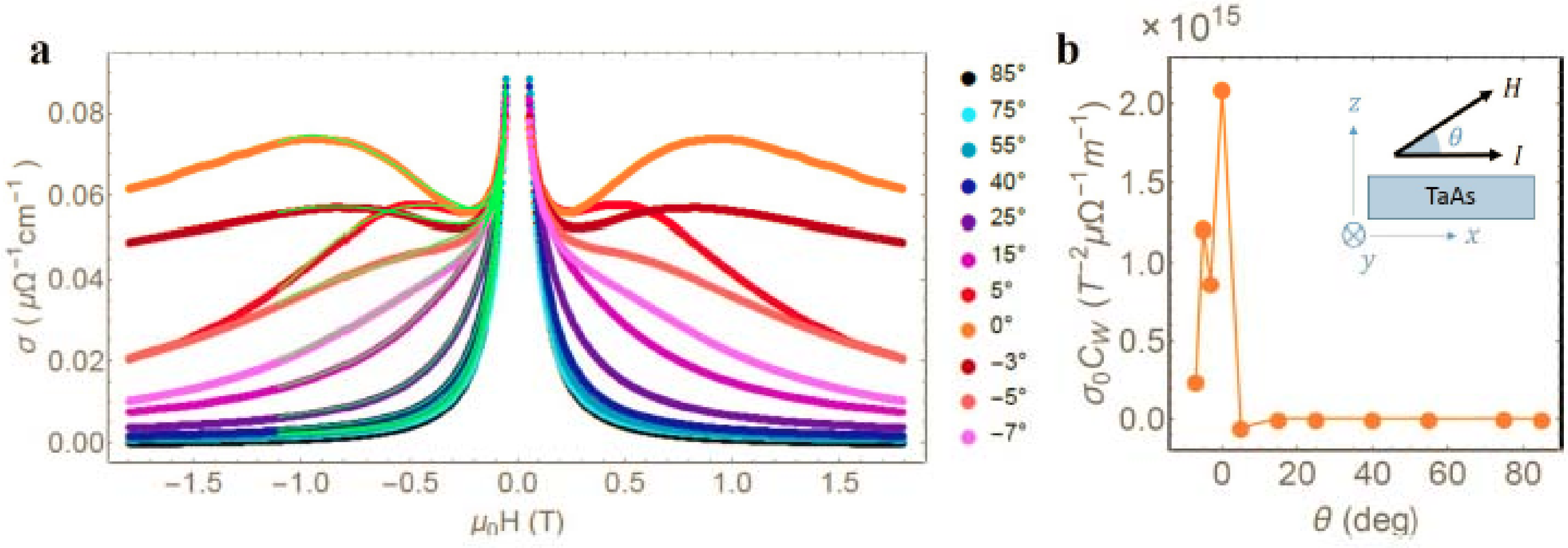


- This Negative LMR (Positive conductance) is extremely sensitive to the angle deviation

# SUMMARY

- We observed first Weyl semimetal TaAs in experiment
- Large MR and strong SdH oscillations
- Negative Longitudinal MR was understood as a Chiral anomaly in TaAs
- Need other candidates of Weyl semimetals and further studies in transport

# PLAN

- Best candidates for studying the e-e interactions beyond QL
- Devices: the key point for observing the exotic chiral-related transport